NASA Contractor Report 172209

NASA-CR-172209
19830027438

MIXED TIME INTEGRATION METHODS FOR TRANSIENT THERMAL ANALYSIS OF STRUCTURES

Wing Kam Liu

NORTHWESTERN UNIVERSITY
Evanston, Illinois 60201

Grant NAG1-210
September 1983

National Aeronautics and
Space Administration

Langley Research Center
Hampton, Virginia 23665

1. INTRODUCTION

Over the last two decades, significant attention has been devoted to the development of lightweight, durable thermal protection systems (TPS) for future space transportation systems. Research programs are currently underway at the Langley Research Center to investigate various metallic TPS concepts [1]. One of the proposed candidates is the titanium multiwall tile (see [2] and references therein for a discussion). Early design procedures of the TPS concept involved both analytical and experimental studies. In particular, a degree of confidence has been established in the TPS concept due to the design studies by Jackson and Dixon [3] and Blair et al. [4].

A titanium multiwall tile consists of alternating layers of superplastically formed dimpled sheets and flat septum sheets of titanium foil. As described in reference [3], this multiwall concept impedes all three modes of heat transfer----conduction, radiation and convection. The superplastically formed dimpled sheets and the long thin conduction path tend to minimize heat conduction. The flat septum sheets of titanium foil impede radiation. The small individual volumes created by the dimpled layers virtually eliminate air convection. The optimal design of such thermal protection systems requires effective techiques in coupled thermal and stress analyses. Finite element methods offer the greatest potential in modeling such complicated problems. However, the resulting semi-discrete equations may involve many thousand degrees of freedom. Since the problem to be solved is transient and nonlinear, the selection of an appropriate time integration method is an essential step in the solution of such a complicated problem. Adelman and Hafka [5] recently conducted a survey study on the performance of explicit and implicit algorithms for transient thermal analysis of structures. Calculations were carried out using the SPAR finite element computer program [6] and

a special purpose finite element program incorporating the GEARB and GEARIB algorithms. Based upon their studies, they concluded that, generally, implicit algorithms are preferable to explicit algorithms for "stiff" problems, though non-convergence and/or wide-banding of the resulting matrix equations may decrease the advantage of the implicit methods.

These difficulties are similar to those found in fluid-structure problems. Over the past few years, several remedies have been proposed for these difficulties. Belytschko and Mullen [7] have proposed an explicit-implicit method where the mesh is partitioned into domains by nodes and the partitions are simultaneously integrated by explicit and implicit methods. Hughes and Liu [8] have proposed an alternate implicit-explicit finite element method where the mesh is partitioned into domains by elements and this element partition concept simplifies the computer-implementation and enhances its compatibility with the general purpose finite element software.

Although the implicit-explicit method has been proven to be very successful in some fluid-structure interaction problems (see e.g., [8-10]), the size and complexity of the program are increased because of the addition of the implicit method. To overcome these difficulties, Belytschko and Mullen [11] have proposed an E^m-E partition, in which explicit time integration is used throughout. However, different time steps within different parts of the mesh can be employed simultaneously. Partitioned and adaptive algorithms for explicit time integration have also been proposed by Belytschko [12].

Recently, Liu and Belytschko [13] put forward a general mixed time implicit-explicit partition procedure within a linear context. It incorporates the mentioned algorithms as special cases and is shown to have better stability properties than that in E^m-E partition [11]. Similar concepts can also be used in transient conduction forced-convection analysis (see Liu and

Lin [14]).

In the present report, these implicit-explicit concepts (nodes and elements) are extended to transient thermal analysis of structures where different time integration methods with different time steps can be used in each element group. The aim of this approach is to achieve the attributes of the various time integration methods.

For example, in transient structural analysis, explicit methods require the size of the time step to be proportional to the length of the shortest element; while in transient thermal analysis, explicit methods require the step size to be porportional to the the square of the length of the shortest element. So it is more advantageous to employ this mixed time implicit-explicit technique for transient thermal analysis of structures since the E^m-E partition proposed in [11,12] is often inefficient for this kind of problem though it is very efficient in structural analysis.

In section 2 the finite element formulation for transient heat conduction is reviewed. In section 3 the mixed time integration procedures viz two element groups "A" and "B" are described. A family of integration partitions can then be deduced by selecting the appropriate definitions for the quantities of "A" and "B". Five useful partitions which are of practical importances are presented. The stability criterion and critical time step estimates are given in sections 4 and 5, respectively. In section 6 the mixed time methods described in section 3 are generalized to NUMEG element groups. A computational algorithm for this mixed time implicit-explicit integration is also presented. In section 7 an illustrative example problem is described to demonstrate the practicability and usefulness of the proposed approach. In addition, the selection of a time integration method and the selection of an element group time step for each group are illustrated. Three numerical

example solutions are presented in section 8 to evaluate the performance (i.e., accuracy and stability behavior, computer storage and solution time, etc.) of these mixed time finite element algorithms. This represents the first comprehensive study of the effectiveness of the proposed methods. Related discussion and conclusions are presented in section 9.

2. FINITE ELEMENT FORMULATION FOR TRANSIENT HEAT CONDUCTION

Consider a body Ω enclosed by surface Γ which consists of two parts: Γ_g and Γ_q. The Cartesian coordinates of the body will be denoted by x_i.

The governing equation for transient heat conduction with constant coefficients is:

$$\theta_{,ii} = \frac{1}{a}\dot{\theta} \qquad \text{in } \Omega\ ,\ i=1,\ldots,NSD \qquad (1)$$

$$\theta = g \qquad \text{for } x_i \text{ on } \Gamma_g \text{ and } t \geq 0 \qquad (2)$$

$$\theta_{,i}n_i + h\theta = q \qquad \text{for } x_i \text{ on } \Gamma_q \text{ and } t \geq 0 \qquad (3)$$

and

$$\theta = \theta_o \qquad \text{for } x_i \text{ in } \Omega \text{ and } t = 0\ . \qquad (4)$$

Here a comma designates a partial derivative with respect to x_i; a superscript dot designates time (t) derivative; n_i is the x_i component of the outward unit normal vector; NSD is the number of space dimensions; a is the thermal diffusivity (the ratio of thermal conductivity to specific heat times density); θ is the temperature; h is the ratio of convective heat transfer coefficient to thermal conductivity; and g, the prescribed boundary temperature; q, the prescribed heat flux and θ_o, the initial temperature are given. Repeated indices denote summations over the appropriate range.

The variational or weak form of equations (1)-(3) with (4) as the initial condition is:

$$(\dot{\theta}\ v) + A(\theta\ v) = (q\ v)_{\Gamma_q} \tag{5}$$

where v is the test function; and

$$(\dot{\theta}\ v) = \int_\Omega \frac{1}{a}\dot{\theta}\ v d\Omega\ , \tag{6}$$

$$A(\theta\ v) = \int_\Omega \theta_{,i} v_{,i} d\Omega + \int_{\Gamma_q} h\theta v\ d\Gamma\ , \tag{7}$$

and

$$(q\ v)_{\Gamma_q} = \int_{\Gamma_q} qv\ d\Gamma\ . \tag{8}$$

The finite element equations are obtained by approximating the trial functions by shape functions (N_i) so that

$$v = \sum_{i=1}^{NEQ} N_i(x_j) d_i(t)\ , \tag{9}$$

$$g = \sum_{1=NEQ+1}^{NUMNP} N_i(x_j) g_i(x_j, t)\ , \tag{10}$$

and

$$\theta = v + g \tag{11}$$

Here NUMNP is the total number of nodal points used in the finite element mesh; and NEQ is the number of trial functions used (for this particular case it is equal to the number of equations to be solved).

The resulting semidiscrete equation for transient heat conduction is

then:

$$\underset{\sim}{\underset{\sim}{M}}\dot{\theta} + \underset{\sim}{\underset{\sim}{K}}\theta = \underset{\sim}{F} , \tag{12}$$

with initial condition

$$\underset{\sim}{\dot{\theta}}(0) = \underset{\sim}{\theta}_o , \tag{13}$$

where the mass matrix,

$$\underset{\sim}{\underset{\sim}{M}} = \lfloor M_{ij} \rfloor = (N_i \quad N_j) = \int_\Omega \frac{1}{a} \quad N_i N_j d\Omega \tag{14}$$

represents the thermal energy stored in the body Ω. The conductivity matrix,

$$\underset{\sim}{\underset{\sim}{K}} = \lfloor K_{ij} \rfloor = A(N_i \quad N_j) = \int_\Omega N_{i,k} N_{j,k} d\Omega + \int_{\Gamma_q} hN_i N_j \, d\Gamma , \tag{15}$$

represents the conductive transfer of energy within the body Ω and the convective transfer of energy across the boundary, Γ_q. The heat load vector,

$$\underset{\sim}{F} = \lfloor F_i \rfloor = (q \; N_i)_{\Gamma_q} - (N_k \; N_i)\dot{g}_k - A(N_k \; N_i) g_k . \tag{16}$$

represents the impressed temperature condition on surface Γ_g and the surface convection on surface Γ_q. $\underset{\sim}{\underset{\sim}{M}}$ and $\underset{\sim}{\underset{\sim}{K}}$ are symmetric and positive definite.

3. MIXED TIME PARTITION PROCEDURES

In this section, mixed time integration methods are employed to solve equations (12) and (13). For the purpose of describing these mixed time integration techniques the mesh is subdivided into element groups A and B, each of which is to be integrated by a different method. Let n be the time step number; $\underset{\sim}{\theta}_n$, $\underset{\sim}{V}_n$ and $\underset{\sim}{F}_n$ be approximations to $\underset{\sim}{\theta}(t_n)$, $\dot{\underset{\sim}{\theta}}(t_n)$ and $\underset{\sim}{F}(t_n)$ respectively. Let $m\Delta t$ and Δt be the time steps used for element group A and element group B respectively, where m is an integer and is greater or equal to 1. A time step cycle ($m\Delta t$) can then be defined by an increment of m substeps with a time step of Δt each, so that one time step cycle is defined by step n to step n+m. The portions of the matrices obtained by assembling element group A and element group B are denoted by superscripts "A" and "B", respectively. Hence it follows that any global matrix is the sum of the two matrices, cf. $\underset{\sim}{M} = \underset{\sim}{M}^A + \underset{\sim}{M}^B$ and $\underset{\sim}{K} = \underset{\sim}{K}^A + \underset{\sim}{K}^B$. Nodes associated with <u>only</u> element group B are denoted by superscript "B", whereas those which are in contact with at least one element of group A are denoted by superscript "A"; nodes which are connected to both group A and group B are designated by "C", so "C" is a subset of "A". To simplify the presentation, we further denote those element matrices associated with at least one node C are denoted by superscript "C", so $\underset{\sim}{M}^C$ and $\underset{\sim}{K}^C$ are subsets of $\underset{\sim}{M}^B$ and $\underset{\sim}{K}^B$ respectively. However, in actual computer implementation this element group is not necessary. With these definitions, $\underset{\sim}{M}^R = \underset{\sim}{M}^A + \underset{\sim}{M}^C$ and $\underset{\sim}{K}^R = \underset{\sim}{K}^A + \underset{\sim}{K}^C$.

Similarly, all vectors are then partitioned accordingly into "A" and "B" parts, cf. $\underset{\sim}{\theta} = (\underset{\sim}{\theta}^A \underset{\sim}{\theta}^B)^T$, $\underset{\sim}{V} = (\underset{\sim}{V}^A \underset{\sim}{V}^B)^T$ and $\underset{\sim}{F} = (\underset{\sim}{F}^A \underset{\sim}{F}^B)^T$. The superscript "T" denotes the transpose. The vector $\underset{\sim}{\theta}$ is sometimes redefined by augmented matrices, $\underset{\sim}{\theta} = \underset{\sim}{\theta}^{*A} + \underset{\sim}{\theta}^{*B}$ where $\theta^{*A} = (\underset{\sim}{\theta}^A \underset{\sim}{0})^T$ and $\underset{\sim}{\theta}^{*B} = (\underset{\sim}{0} \underset{\sim}{\theta}^B)^T$. Similar definitions are used for $\underset{\sim}{V}$ and $\underset{\sim}{F}$. Any nonzero terms in $\underset{\sim}{F}^A$ obtained in a compu-

tation of $\underset{\sim}{F}^{*B}$ are neglected; they are assumed to be zero.

As an example, consider a one dimensional bar with two groups of material A and B depicted in figure 1. Group B material has higher conductivity than group A that a smaller time step (Δt) is required for group B whereas a larger time step ($m\Delta t$) can be used for group A. This mesh consists of 8 nodes and 7 elements. Then the set of nodes "A" will be 1,2,3,4,5; the set of nodes "B" will be 6,7,8; and the set of nodes "C" will be 5.

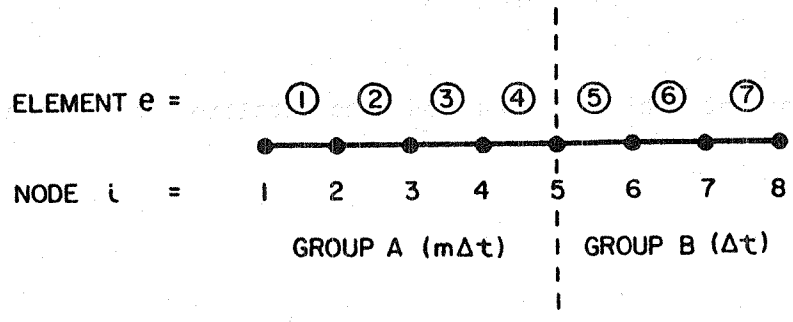

Fig. 1. One dimensional mesh with two element groups

Let $\underset{\sim}{M}^{e}$, $\underset{\sim}{K}^{e}$ and $\underset{\sim}{F}^{e}$ be the thermal energy stored in the eth element, the conductive transfer of energy in the eth element including the convective transfer of energy across the element boundary and the heat load contributions to the global arrays respectively, then

$$\underset{\sim}{M}^{A} = \sum_{e=1}^{4} \underset{\sim}{M}^{e} \quad , \qquad \underset{\sim}{K}^{A} = \sum_{e=1}^{4} \underset{\sim}{K}^{e} \quad , \qquad \underset{\sim}{F}^{A} = \sum_{e=1}^{4} \underset{\sim}{F}^{e} \quad ;$$

$$\underset{\sim}{M}^{B} = \sum_{e=5}^{7} \underset{\sim}{M}^{e} \quad , \qquad \underset{\sim}{K}^{B} = \sum_{e=5}^{7} \underset{\sim}{K}^{e} \quad , \qquad \underset{\sim}{F}^{B} = \sum_{e=5}^{7} \underset{\sim}{F}^{e} \quad ;$$

$$\underset{\sim}{M}^{C} = \underset{\sim}{M}^{5} \quad , \qquad \underset{\sim}{K}^{C} = \underset{\sim}{K}^{5} \quad , \qquad \underset{\sim}{F}^{C} = \underset{\sim}{F}^{5} \quad ;$$

and

$$\underset{\sim}{M}^R = \sum_{e=1}^{5} \underset{\sim}{M}^e \quad , \qquad \underset{\sim}{K}^R = \sum_{e=1}^{5} \underset{\sim}{K}^e \quad , \qquad \underset{\sim}{F}^R = \sum_{e=1}^{5} \underset{\sim}{F}^e \quad .$$

If we let P_i^{*B} be the ith component of the global assembled vector $\underset{\sim}{P}^{*B}$ then

$$\underset{\sim}{P}^{*B} = (0,0,0,0,P_5 \equiv 0, P_6, P_7, P_8) \quad .$$

With these definitions, the mixed time partition is given as follows.

Governing equation

for j=0,m;

$$\underset{\sim\sim}{M}\underset{\sim}{V}_{n+j} + \underset{\sim}{K}^R \hat{\underset{\sim}{\theta}}^{*A}_{n+j} + \underset{\sim}{K}^B \hat{\underset{\sim}{\theta}}^{*B}_{n+j} = \underset{\sim}{F}_{n+j} \tag{17}$$

and

for j=1,...,m-1;

$$\underset{\sim}{M}^B \underset{\sim}{V}^{*B}_{n+j} + \underset{\sim}{K}^B \hat{\underset{\sim}{\theta}}^{*B}_{n+j} + \underset{\sim}{K}^C \hat{\underset{\sim}{\theta}}^{*A}_{n+j} = \underset{\sim}{F}^{*B}_{n+j} \tag{18}$$

where $\hat{\underset{\sim}{\theta}}^{*x}_{n+j}$ is a suitable extrapolator (and/or interpolator) of $\underset{\sim}{\theta}^{*x}_n$ (and/or $\underset{\sim}{\theta}^{*x}_{n+m}$) for x=A and B. In actual computation, equation (18) is implicitly included in equation (17); and for j=1,...,m-1 no quantities of A are being solved. A family of integration partitions can then be deduced from equations (17) to (18) if $\underset{\sim}{M}$ is assumed to be lumped. Some members which are of practical importances are shown in table 1.

Table 1

Designation	Time Integration In Element Group A	Time Integration In Element Group B	Extrapolator/Interpolator	
			Node A	Node B
E-E	explicit with Δt	explicit with Δt	$\underset{\sim}{\theta}^{*A}_{n}$	$\underset{\sim}{\theta}^{*B}_{n}$
mE-E	explicit with $m\Delta t$	explicit with Δt	$\underset{\sim}{\theta}^{*A}_{n}$	$\underset{\sim}{\theta}^{*B}_{n}$
mE-I	implicit with $m\Delta t$	explicit with Δt	$\underset{\sim}{\theta}^{*A}_{n+m}$	$\underset{\sim}{\theta}^{*B}_{n}$
E-I	implicit with Δt	explicit with Δt	$\underset{\sim}{\theta}^{*A}_{n+1}$	$\underset{\sim}{\theta}^{*B}_{n}$
I-I	implicit with Δt	implicit with Δt	$\underset{\sim}{\theta}^{*A}_{n+1}$	$\underset{\sim}{\theta}^{*B}_{n+1}$

For purposes of describing the computer implementation and stability analysis, the modified generalized trapezoidal rule will be used to carry out the time temporary discretization of equations (17) and (18) though other implicit integration methods can also be used.

● Modified generalized trapezoidal rule

for $j=1,\ldots,m$;

$$\underset{\sim}{\tilde{\theta}}^{A}_{n+j} = \underset{\sim}{\theta}^{A}_{n} + (1-\alpha)j\Delta t\ \underset{\sim}{V}^{A}_{n} \tag{19}$$

for $1 \leqslant j < m$ define the set "C" only,

$$\underset{\sim}{\tilde{\theta}}^{B}_{n+j} = \underset{\sim}{\theta}^{B}_{n+j-1} + (1-\alpha)\Delta t\ \underset{\sim}{V}^{B}_{n+j-1}\ , \tag{20}$$

$$\underset{\sim}{\theta}^{A}_{n+m} = \underset{\sim}{\tilde{\theta}}^{A}_{n+m} + \alpha m\ \Delta t\ \underset{\sim}{V}^{A}_{n+m}\ , \tag{21}$$

and

$$\underset{\sim}{\theta}^{B}_{n+j} = \underset{\sim}{\tilde{\theta}}^{B}_{n+j} + \alpha\Delta t \; \underset{\sim}{V}^{B}_{n+j} \; . \tag{22}$$

In the above equations, α is a free parameter which governs the stability and accuracy of the method. Some useful partitions which have been depicted in table 1 are illustrated below.

Example 1: E-E Partition

In this case, m=1, $\underset{\sim}{\theta}^{x}_{n+1} \equiv \underset{\sim}{\tilde{\theta}}^{x}_{n+1}$ for x=A and B. Equations (17) to (18) reduce to:

$$\underset{\sim\sim}{M}\underset{\sim}{V}_{n+1} + \underset{\sim\sim}{K}\underset{\sim}{\tilde{\theta}}_{n+1} = \underset{\sim}{F}_{n+1} \; , \tag{23}$$

$$\underset{\sim}{\tilde{\theta}}_{n+1} = \underset{\sim}{\theta}_{n} + (1-\alpha)\Delta t \; \underset{\sim}{V}_{n} \; , \tag{24}$$

and

$$\underset{\sim}{\theta}_{n+1} = \underset{\sim}{\tilde{\theta}}_{n+1} + \alpha\Delta t \; \underset{\sim}{V}_{n+1} \; . \tag{25}$$

Equations (23) to (25) represent the predictor-corrector explicit algorithms with equation (24) as the predictor and equation (25) as the corrector.

Example 2: mE-E Partition

In this case, m > 1, $\underset{\sim}{\hat{\theta}}^{A}_{n+j} \equiv \underset{\sim}{\tilde{\theta}}^{A}_{n+j}$ and $\underset{\sim}{\hat{\theta}}^{B}_{n+j} \equiv \underset{\sim}{\tilde{\theta}}^{B}_{n+j}$. Equations (17) to (22) reduce to:

PREDICTOR PHASE:

equation (19) (26)

and

equation (20) (27)

GOVERNING EQUATIONS:

equation (17) (28)

and

equation (18) (29)

CORRECTOR PHASE:

equation (21) (30)

and

equation (22) (31)

Example 3: mE-I partition

In this case, $m > 1$; in equation (17), $\hat{\underset{\sim}{\theta}}^{A}_{n+j} \equiv \underset{\sim}{\theta}^{A}_{n+m}$ for element group A only, $\hat{\underset{\sim}{\theta}}^{A}_{n+j} \equiv \tilde{\underset{\sim}{\theta}}^{A}_{n+m}$ for the portion which is related to $\underset{\sim}{K}^{C}$ for $j=0$ and m.

This is done automatically if element group A is defined to be the implicit element group and element group B is defined to be the explicit element group. $\hat{\theta}^{A}_{n+j} \equiv \tilde{\theta}^{A}_{n+j}$ for $1 \leq j < m$; and $\hat{\theta}^{B}_{n+j} \equiv \tilde{\theta}^{B}_{n+j}$ for $1 \leq j \leq m$. Equations (17) to (22) reduce to:

PREDICTOR PHASE:

equation (19) (32)

and

equation (20) (33)

GOVERNING EQUATIONS:

for j=0,m;

$$M V_{n+j} + K^{A} \theta^{*A}_{n+j} + K^{B} \tilde{\theta}_{n+j} = F_{n+j} \,, \tag{34}$$

and

for j=1,...,m-1;

$$M^{B} V^{*B}_{n+j} + K^{B} \tilde{\theta}^{*B}_{n+j} + K^{C} \tilde{\theta}^{*A}_{n+j} = F^{*B}_{n+j} \,, \tag{35}$$

CORRECTOR PHASE:

equation (21) (36)

equation (22) (37)

Example 4: E-I partition

This is a special case of example 3. Equations (17) to (22) reduce to:

$$\underset{\sim}{\underset{\sim}{M}}\underset{\sim}{V}_{n+1} + \underset{\sim}{\underset{\sim}{K}}^{A}\underset{\sim}{\theta}_{n+1} + \underset{\sim}{\underset{\sim}{K}}^{B}\underset{\sim}{\tilde{\theta}}_{n+1} = \underset{\sim}{F}_{n+1} \tag{38}$$

$$\underset{\sim}{\tilde{\theta}}_{n+1} = \underset{\sim}{\theta}_{n} + (1-\alpha)\Delta t\ \underset{\sim}{V}_{n} \tag{39}$$

$$\underset{\sim}{\theta}_{n+1} = \underset{\sim}{\tilde{\theta}}_{n+1} + \alpha\Delta t\ \underset{\sim}{V}_{n+1} \tag{40}$$

Equations (38) to (40) represent the implicit-explicit algorithms developed by Hughes and Liu (see e.g., [8,10]) in which equation (39) is the predictor and equation (40) is the corrector.

Example 5: I-I partition

In this case, $m=1$, $\underset{\sim}{\hat{\theta}}^{A}_{n+1} \equiv \underset{\sim}{\theta}^{A}_{n+1}$ and $\underset{\sim}{\hat{\theta}}^{B}_{n+1} \equiv \underset{\sim}{\theta}^{B}_{n+1}$. Equation (17) to (22) reduce to the usual implicit formulation and it is:

$$\underset{\sim}{\underset{\sim}{M}}\underset{\sim}{V}_{n+1} + \underset{\sim}{\underset{\sim}{K}}\underset{\sim}{\theta}_{n+1} = \underset{\sim}{F}_{n+1} \tag{41}$$

$$\underset{\sim}{\tilde{\theta}}_{n+1} = \underset{\sim}{\theta}_{n} + (1-\alpha)\Delta t\ \underset{\sim}{V}_{n} \tag{42}$$

$$\underset{\sim}{\theta}_{n+1} = \underset{\sim}{\tilde{\theta}}_{n+1} + \alpha\Delta t\ \underset{\sim}{V}_{n+1} \tag{43}$$

4. STABILITY CRITERION

The stability characteristics of these mixed time partition algorithms can be deduced using an energy balance technique (see [8] for a discussion). The analysis is restricted to the case in which $\underset{\sim}{F}=\underset{\sim}{0}$ and all capacitance matrices are lumped. To simplify the subsequent writing, the following notations will be used.

$$\lfloor \underset{\sim}{x}_{n+m} \rfloor = \underset{\sim}{x}_{n+m} - \underset{\sim}{x}_{n} \ , \tag{44}$$

$$\langle \underset{\sim}{x}_{n+m} \rangle = (\underset{\sim}{x}_{n+m} + \underset{\sim}{x}_{n})/2 \ , \tag{45}$$

$$\lfloor \underset{\sim}{x}_{n+j} \rfloor = \underset{\sim}{x}_{n+j+1} - \underset{\sim}{x}_{n+j} \ , \tag{46}$$

and for $j=0,1,\ldots,m-1$

$$\langle \underset{\sim}{x}_{n+j} \rangle = (\underset{\sim}{x}_{n+j+1} + \underset{\sim}{x}_{n+j})/2 \ . \tag{47}$$

Assume:

1. $\langle \underset{\sim}{V}^{*A}_{n+m} \rangle^T \underset{\sim}{K}^C \langle \underset{\sim}{V}^{*A}_{n+m} \rangle / \underset{\sim}{z}^{*B^T} \underset{\sim}{K}^C \underset{\sim}{z}^{*B} \geq 1/m^2$, where

$$\underset{\sim}{z}^{*B} = \underset{\sim}{V}^{*B}_{n} + \sum_{j=1}^{m-2} \langle \underset{\sim}{V}^{*B}_{n+j} \rangle \ ; \tag{48}$$

2. $\langle \underset{\sim}{V}^{*B}_{n} \rangle^T \underset{\sim}{K}^C \langle \underset{\sim}{V}^{*B}_{n} \rangle / \underset{\sim}{V}^{*A^T}_{n} \underset{\sim}{K}^C \underset{\sim}{V}^{*A}_{n} \geq (1+(m-1)\alpha)^2 \ ;$ (49)

3. $\langle \underset{\sim}{V}^{*B}_{n+j} \rangle^T \underset{\sim}{K}^C \langle \underset{\sim}{V}^{*B}_{n+j} \rangle / \underset{\sim}{V}^{*A^T}_{n} \underset{\sim}{K}^C \underset{\sim}{V}^{*A}_{n} \geq (1-\alpha)^2$ for

$$j=1,\ldots,m-1 \ ; \tag{50}$$

and let:

4. $$S_n = \underset{\sim}{V}^{*A^T}_{n} \ \underset{\sim}{M}^{*R} \ \underset{\sim}{V}^{*A}_{n} + \underset{\sim}{V}^{*B^T}_{n} \ \underset{\sim}{M}^{*B} \ \underset{\sim}{V}^{*B}_{n} \geq 0 \ ; \tag{51}$$

5. $$P^A_{n+m} = \langle \underset{\sim}{V}^{*A}_{n+m} \rangle^T \ \underset{\sim}{K}^A \ \langle \underset{\sim}{V}^{*A}_{n+m} \rangle \geq 0 \ ; \tag{52}$$

6. $$P^B_{n+j} = \langle \underset{\sim}{V}^{*B}_{n+j} \rangle^T \ \underset{\sim}{K}^{\bar{B}} \ \langle \underset{\sim}{V}^{*B}_{n+j} \rangle \geq 0 \ ; \tag{53}$$

the energy expression of these mixed time partition procedures can be shown to be:

$$S_{n+m} \leq S_n - 2m\Delta t \ P^A_{n+m} - 2\Delta t \sum_{j=0}^{m-1} P^B_{n+j} \ . \tag{54}$$

Here, $\underset{\sim}{K}^{\bar{B}} = \underset{\sim}{K}^B - \underset{\sim}{K}^C$ and the stability is governed by $\underset{\sim}{M}^{*R}$ and $\underset{\sim}{M}^{*B}$ provided $\alpha \geq 1/2$. Let

$$\underset{\sim}{Q}^X_j = \underset{\sim}{M}^X - 1/2j\Delta t \ \underset{\sim}{K}^X \ , \tag{55}$$

and

$$\underset{\sim}{W}^X_j = \underset{\sim}{M}^X + (\alpha - 1/2)j\Delta t \ \underset{\sim}{K}^X \ ; \tag{56}$$

the definitions of $\underset{\sim}{M}^{*R}$ and $\underset{\sim}{M}^{*B}$ for the five cases discussed in section 3 are:

Example 1: E-E partition

$$\underset{\sim}{M}^{*R} = \underset{\sim}{Q}_1^R \quad , \quad \text{and} \quad \underset{\sim}{M}^{*B} = \underset{\sim}{Q}_1^B \quad . \tag{57}$$

Example 2: mE-E partition

$$\underset{\sim}{M}^{*R} = \underset{\sim}{Q}_m^R \quad , \quad \text{and} \quad \underset{\sim}{M}^{*B} = \underset{\sim}{Q}_1^B \quad . \tag{58}$$

Example 3: mE-I partition

$$\underset{\sim}{M}^{*R} = \underset{\sim}{W}_m^A + \underset{\sim}{Q}_m^C \quad , \quad \text{and} \quad \underset{\sim}{M}^{*B} = \underset{\sim}{Q}_1^B \quad . \tag{59}$$

Example 4: E-I partition

$$\underset{\sim}{M}^{*R} = \underset{\sim}{W}_1^A + \underset{\sim}{Q}_1^C \quad , \quad \text{and} \quad \underset{\sim}{M}^{*B} = \underset{\sim}{Q}_1^B \quad . \tag{60}$$

Example 5: I-I partition

$$\underset{\sim}{M}^{*R} = \underset{\sim}{W}_1^R \quad , \quad \text{and} \quad \underset{\sim}{M}^{*R} = \underset{\sim}{W}_1^B \tag{61}$$

These mixed time partition procedures are stable if $\alpha \geq 1/2$ and $\underset{\sim}{M}^{*R}$ and $\underset{\sim}{M}^{*B}$ are both positive definite. A summary of the results is as follows:

Example 1: E-E partition

$$\Omega_{crit}^A = \Omega_{crit}^B \leq 2 \quad . \tag{62}$$

Example 2: mE-E partition

$$\Omega^{mA}_{crit} = \Omega^{mC}_{crit} \leq 2 \quad , \quad \text{and} \quad \Omega^{B}_{crit} \leq 2 \quad . \tag{63}$$

Example 3: mE-I partition

$$\Omega^{mC}_{crit} \leq 2 \quad , \quad \text{and} \quad \Omega^{B}_{crit} \leq 2 \quad . \tag{64}$$

Example 4: E-I partition

$$\Omega^{C}_{crit} \leq 2 \quad , \quad \text{and} \quad \Omega^{B}_{crit} \leq 2 \quad . \tag{65}$$

Example 5: I-I partition

unconditionally stable. (66)

In equations (62) to (65), Ω^{jx} is defined to be $j\Delta t\ \lambda^{x}_{crit}$; where λ^{x}_{crit} denotes a typical eigenvalue of the eigenproblem

$$\underset{\sim}{M}^{x}\dot{\underset{\sim}{\theta}} + \underset{\sim}{K}^{x}\underset{\sim}{\theta} = \underset{\sim}{0} \tag{67}$$

5. CRITICAL TIME STEP ESTIMATES FOR BILINEAR QUADRILATERAL ELEMENT

For the one point quadrature element, there are four eigenvalues of which only two of them are nonzero. One of these zero eigenvalues can be removed if the stabilization stiffness is added to the one point quadrature stiffness. This third eigenvalue can be shown to be bounded between the other two nonzero eigenvalues. In particular, for the case of a rectangular element, these three eigenvalues are identical to those three obtained by using a two by two quadrature element. Hence a computationally-useful method of estimating the critical time step for linear quadrilaterical element can easily be derived for the mixed time methods.

Following the previous section, $\Delta t_{crit} \leq 2/\lambda_{max}$ is the critical time step restriction and λ_{max} is the maximum eigenvalue of the e^{th} element subjected to insulated boundary conditions.

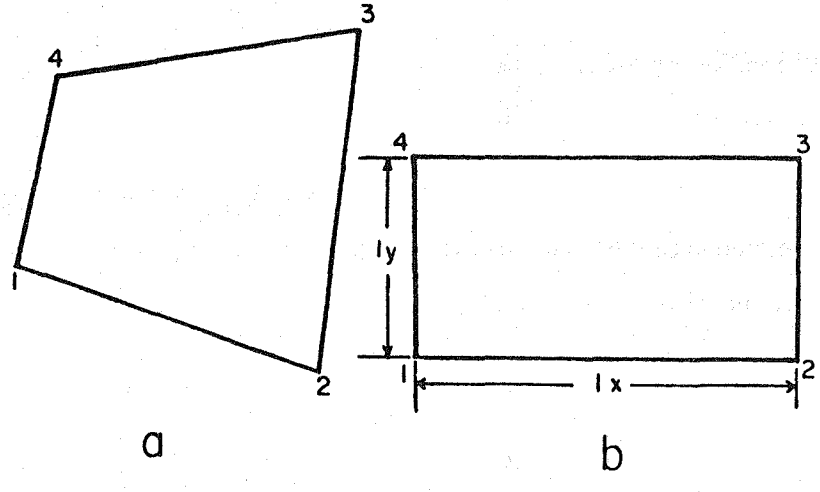

Fig. 2(a). Arbitrary four-node quadrilateral element; (b) rectangular element

For an arbitrary four node quadrilateral as shown in Fig. 2a, Let

$$\underset{\sim}{x}^T = (x_1, x_2, x_3, x_4),$$

and

$$\underline{y}^T = (y_1, y_2, y_3, y_4),$$

are the x and y coordinates of the four nodes. Define

$$x_{IJ} = x_I - x_J,$$

and for I,J=1,...,4 .

$$y_{IJ} = y_I - y_J,$$

Let

$$X = y_{24}^2 + x_{42}^2,$$

$$Y = y_{31}^2 + x_{13}^2,$$

$$Z = -(y_{24}y_{31} + x_{42}x_{13}),$$

and A is the area of the quadrilateral. It can be shown that

$$\Delta t_{crit} \leq \min\left\{\mu \frac{2A^2}{a\{(X+Y) \pm \sqrt{[(X-Y)^2+4Z^2]}\}}\right\} \tag{68}$$

where a is the thermal diffusivity and μ is between 0.95 and 1.0. A numerical study of the eigenvalues of the various shapes (for all practical purposes) two by two quadrature elements has been performed. It is found empirically that μ can be picked to be 0.95 if the element is really skewed and μ can be picked to be 1.0 if the element is rectangular. In the special case of a rectangular element (i.e., with μ=1.0),

$$\Delta t_{crit} \leq \min\left\{\frac{\ell_x^2}{2a}, \frac{\ell_y^2}{2a}\right\}, \tag{69}$$

where ℓ_x and ℓ_y are defined in Fig. 2b.

6. IMPLEMENTATION ASPECTS

In this section, the mixed time integration methods described in section 3 are generalized to NUMEG element groups. Different time integration methods (implicit/explicit) with different time steps can be used in each element group. Let Δt_{NEG} and T_{NEG} be the element group time step and element group time respectively for NEG = 1,...,NUMEG. There are NUMEL elements in each element group, and Δt denote the minimum time step amount all these element groups. In this formulation all element group time steps are required to be integer multiples of Δt and the time steps for adjacent groups are integer multiples of each other. If a physical situation occurs dictating the use of adjacent implicit groups they must be combined into one group with the time step equal to the smaller of the two groups. In addition, for each implicit group, that element group time step must be greater than those of the adjacent explicit groups. The main advantage of this m_1 implicit - m_2 explicit - m_3 implicit -... etc., technique is to minimize the semi-bandwidth of complicated problems especially in the three-dimensional case. To illustrate the idea, consider the one dimensional mesh shown in Fig. 3. It consists of NUMEG element groups and NUMNP nodes. In this case NUMEG is equal to 4 and NUMNP is equal to 12. Node 1 is assumed to be an essential boundary

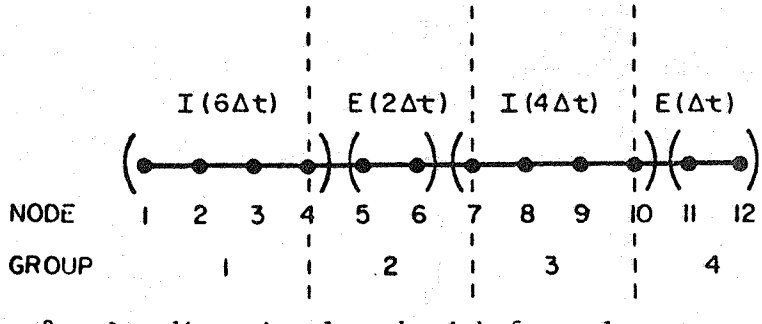

Fig. 3. One dimensional mesh with four element groups

condition node so that the number of equations, NEQ, is equal to 11. The

essence of the present development can be deduced graphically by considering the solution procedures of the matrix equations. The "active column equation solver" is the key to the success of this technique (see [8,13] for a description of this equation solver). The profile of the effective stiffness matrix $\underset{\sim}{K}^*$ of this one dimensional mesh is shown in Fig. 4. It can be observed

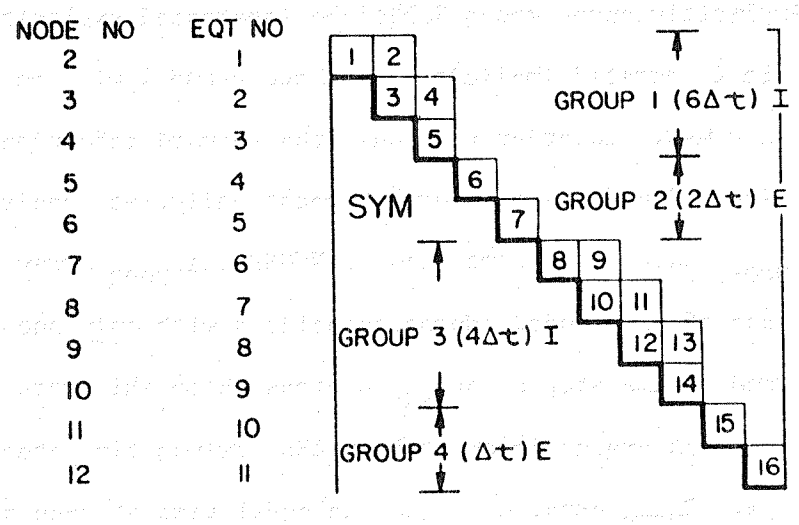

Fig. 4. Profile of the effective stiffness matrix

from Fig. 4 the following:

Group 1: implicit with $\Delta t_1 = 6\Delta t$, five words of storage (1-5), 3 elements and 3 equations.

Group 2: explicit with $\Delta t_2 = 2\Delta t$, two words of storage (6-7), 3 elements and 2 equations.

Group 3: implicit with $\Delta t_3 = 4\Delta t$, seven words of storage (8-14), 3 elements and 4 equations.

Group 4: explicit with $\Delta t_4 = \Delta t$, two words of storage (15-16), 2 elements and 2 equations.

The equation systems of each element group are uncoupled and hence each group can be integrated at its own group time step. For example, assume the effective stiffness matrix $\underset{\sim}{K}^*$ is formed and factorized once. Since each group has its own time clock that in a time interval of $6\Delta t$, group 1 will be integrated implicitly once, group 2 will be integrated explicitly three times, group 3 will be integrated implicitly once and group 4 will be integrated explicitly six times. In order to handle the forward reduction and backsubstitution and update procedures automatically, we required two arrays Δt_{NODE} and T_{NODE}, each has a dimension of NUMNP. Δt_{NODE} array contains the nodal time steps of each node. Nodes associated with only one element group NEG are assigned a time step of Δt_{NEG}, whereas those which are in common to other element groups are assigned to have the maximum time step amount the adjacent groups. T_{NODE} array contains the nodal time of each node. From these two arrays (Δt_{NODE} and T_{NODE}) and the boundary condition codes, another time step array Δt_{NEQ} and an equation time array T_{NEQ} of the equation systems can then be generated. Both Δt_{NEQ} and T_{NEQ} have dimensions of NEQ. It is required further a master time T_M which is incremented by the smallest time step Δt. For this particular example the Δt_{NODE} and Δt_{NEQ} arrays are:

$$\Delta t_{NODE} = (6\Delta t, 6\Delta t, 6\Delta t, 6\Delta t, 2\Delta t, 2\Delta t, 4\Delta t, 4\Delta t, 4\Delta t, 4\Delta t, \Delta t, \Delta t) \ ;$$

and

$$\Delta t_{NEQ} = (6\Delta t, 6\Delta t, 6\Delta t, 2\Delta t, 2\Delta t, 4\Delta t, 4\Delta t, 4\Delta t, 4\Delta t, \Delta t, \Delta t) \ .$$

The T_{NODE} and T_{NEQ} arrays are incremented by time steps of Δt_{NODE} and Δt_{NEQ} respectively. With these definitions, the generalized mixed time integration is to proceed over the time interval $[0, T_{max}]$. The procedures are as follows:

1. Initialization. Set T_M, T_{NEG}, T_{NODE} and $T_{NEQ}=0$, and define the initial data $\underset{\sim}{\theta}_o$ and $\underset{\sim}{V}_o$

2. Form and factorize $\underset{\sim}{K}^*$ where

$$\underset{\sim}{K}^* = \sum_{NEG=1}^{NUMEG} \underset{\sim}{K}^{*NEG},$$

$$\underset{\sim}{K}^{*NEG} = \sum_{e=1}^{NEMEL} \underset{\sim}{K}^{*e},$$

$$\underset{\sim}{K}^{*e} = \underset{\sim}{M}^e + \alpha\Delta t_{NEG}\underset{\sim}{K}^e \quad \text{if implicit,}$$

and

$$\underset{\sim}{K}^{*e} = \underset{\sim}{M}^e \text{ if explicit (lumped capitance matrix is assumed).}$$

3. Time step loop.

4. $T_M \overset{\dagger}{\leftarrow} T_M + \Delta t$, if $T_M \geq T_{MAX}$ stop.

5. Set $\underset{\sim}{F}^* = \alpha\Delta t_{NEQ}\, \underset{\sim}{F}^{DISCRETE}$.

6. Loop on element groups NEG=1,...,NUMEG;

If $T_{NEG} + \Delta t_{NEG} - T_M > Torr$[††] go to 6b.

7. Loop on elements e=1,...,NUMEL;

7a. Define predictor values $\tilde{\underset{\sim}{\theta}}^e$;

If $T^e_{NODE} + \Delta t^e_{NODE} - T_M \leq Torr$,

Then $\tilde{\underset{\sim}{\theta}}^e = \underset{\sim}{\theta}^e_{NODE} + (1-\alpha)\Delta t^e_{NODE}\, \underset{\sim}{V}^e_{NODE}$.

Otherwise $\tilde{\underset{\sim}{\theta}}^e = \underset{\sim}{\theta}^e_{NODE} + (1-\alpha)(T_M - T^e_{NODE})\underset{\sim}{V}^e_{NODE}$.

[†] "←" means "is replaced by".

[††] we use Torr=1.0E-9.

7b. From element effective force $\underset{\sim}{f}^{*e}$.

$\underset{\sim}{f}^{*e} = \underset{\sim}{M}^{e}\underset{\sim}{\ddot{\theta}}^{e}$ if implicit,

and

$\underset{\sim}{f}^{*e} = \underset{\sim}{M}^{e}\underset{\sim}{\ddot{\theta}}^{e} - \alpha \underset{\sim}{W}\, \underset{\sim}{K}^{e}\underset{\sim}{\dot{\theta}}^{e}$ if explicit,

where

$\underset{\sim}{W}$ = diagonal matrix with Δt^{e}_{NODE} along the diagonals.

7c. Sum up effective force from elemental contributions

$\underset{\sim}{F}^{*} \leftarrow \underset{\sim}{F}^{*} + \underset{\sim}{f}^{*e}$

7d. End of element loop.

6a. Update T_{NEG}.

$T_{NEG} = T_{NEG} + \Delta t_{NEG}$

6b. End of element group loop.

8. Solve for $\underset{\sim}{\ddot{\theta}}$. (In order to enhance the efficiency of these mixed time methods, the active column equation solver used in [8,13] is modified in the forward reduction and backsubstitution procedures as follows:)

8a. Loop on equation number N=1,...,NEQ;

If $T^{N}_{NEQ} + \Delta t^{N}_{NEQ} - T_{M} >$ Torr go to 8b.

Forward reduction and backsubstitution for equation N.

8b. End of equation number loop.

9. Update $\underset{\sim}{V}$ and $\underset{\sim}{\dot{\theta}}$;

9a. Loop on N=1,...,NUMNP;

If $T^{N}_{NODE} + \Delta t^{N}_{NODE} - T_{M} >$ Torr go to 9b.

$\underset{\sim}{\ddot{\theta}}^{N} \leftarrow$ solution from step 8.

$\underset{\sim}{V}^{N} \leftarrow (\underset{\sim}{\dot{\theta}}^{N} - \underset{\sim}{\tilde{\dot{\theta}}}^{N})/\alpha\Delta t^{N}_{NODE}$.

9b. End of nodal number loop.

10. Update T_{NODE};

10a. Loop on N=1,...,NUMNP;

If $T^e_{NODE} + \Delta t^e_{NODE} - T_M >$ Torr go to 10b.

$T^e_{NODE} \leftarrow T^e_{NODE} + \Delta t^e_{NODE}$.

10b. End of nodal number loop.

11. Update T_{NEQ};

11a. Loop on N=1,...,NEQ;

If $T^N_{NEQ} + \Delta t^N_{NEQ} - T_M >$ Torr go to 11b.

$T^N_{NEQ} \leftarrow T^N_{NEQ} + \Delta t^N_{NEQ}$

11b. End of equation number loop.

3a. End of time step loop.

A corresponding flowchart of the above procedures is shown on the next few pages.

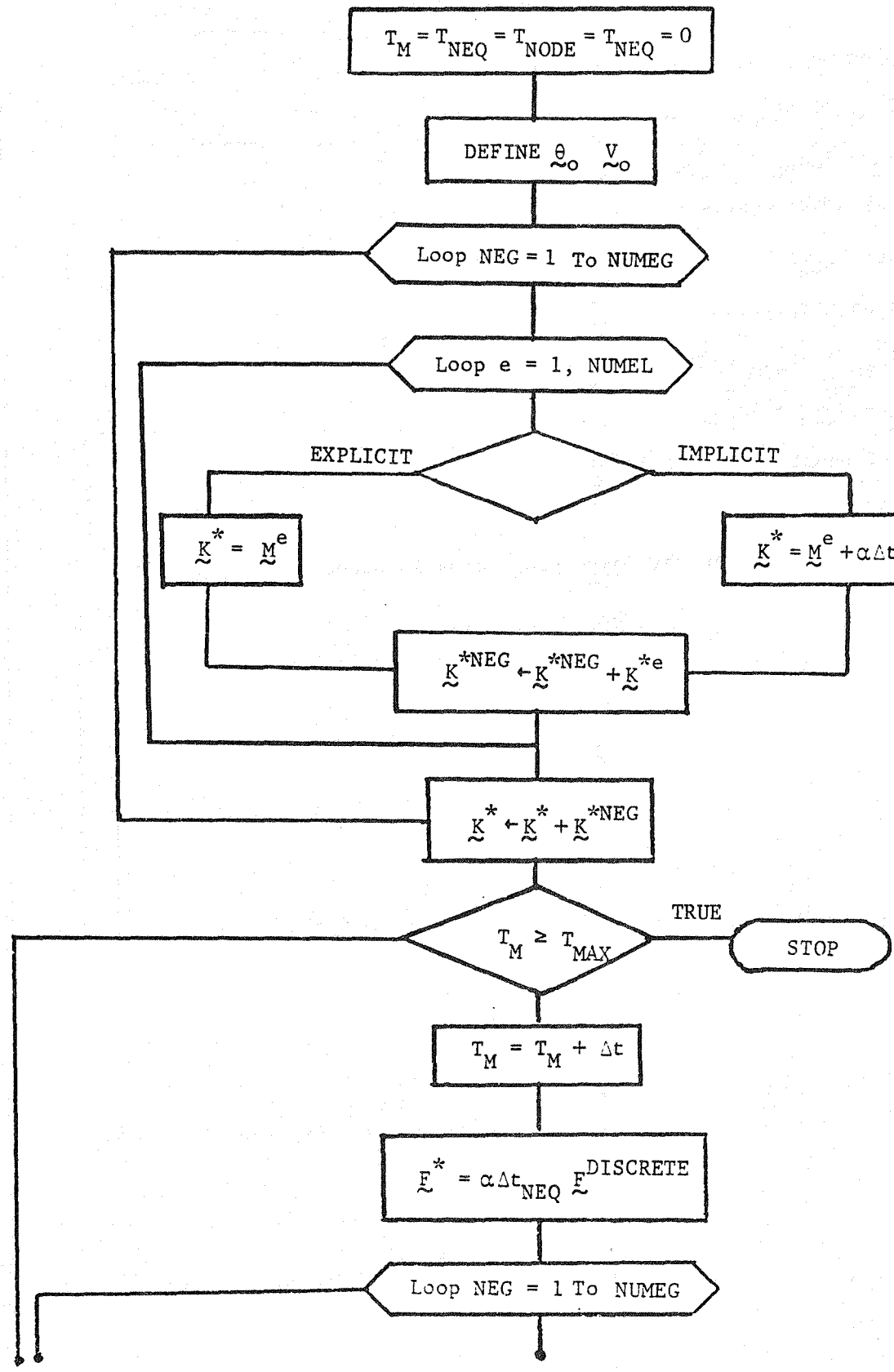
$T_M = T_{NEQ} = T_{NODE} = T_{NEQ} = 0$
DEFINE $\underset{\sim}{\theta}_o$ $\underset{\sim}{V}_o$
Loop NEG = 1 To NUMEG
Loop e = 1, NUMEL
EXPLICIT
IMPLICIT
$\underset{\sim}{K}^* = \underset{\sim}{M}^e$
$\underset{\sim}{K}^* = \underset{\sim}{M}^e + \alpha\Delta t_{NEG}\underset{\sim}{K}^e$
$\underset{\sim}{K}^{*NEG} \leftarrow \underset{\sim}{K}^{*NEG} + \underset{\sim}{K}^{*e}$
$\underset{\sim}{K}^* \leftarrow \underset{\sim}{K}^* + \underset{\sim}{K}^{*NEG}$
$T_M \geq T_{MAX}$
TRUE
STOP
$T_M = T_M + \Delta t$
$\underset{\sim}{F}^* = \alpha\Delta t_{NEQ}\underset{\sim}{F}^{DISCRETE}$
Loop NEG = 1 To NUMEG

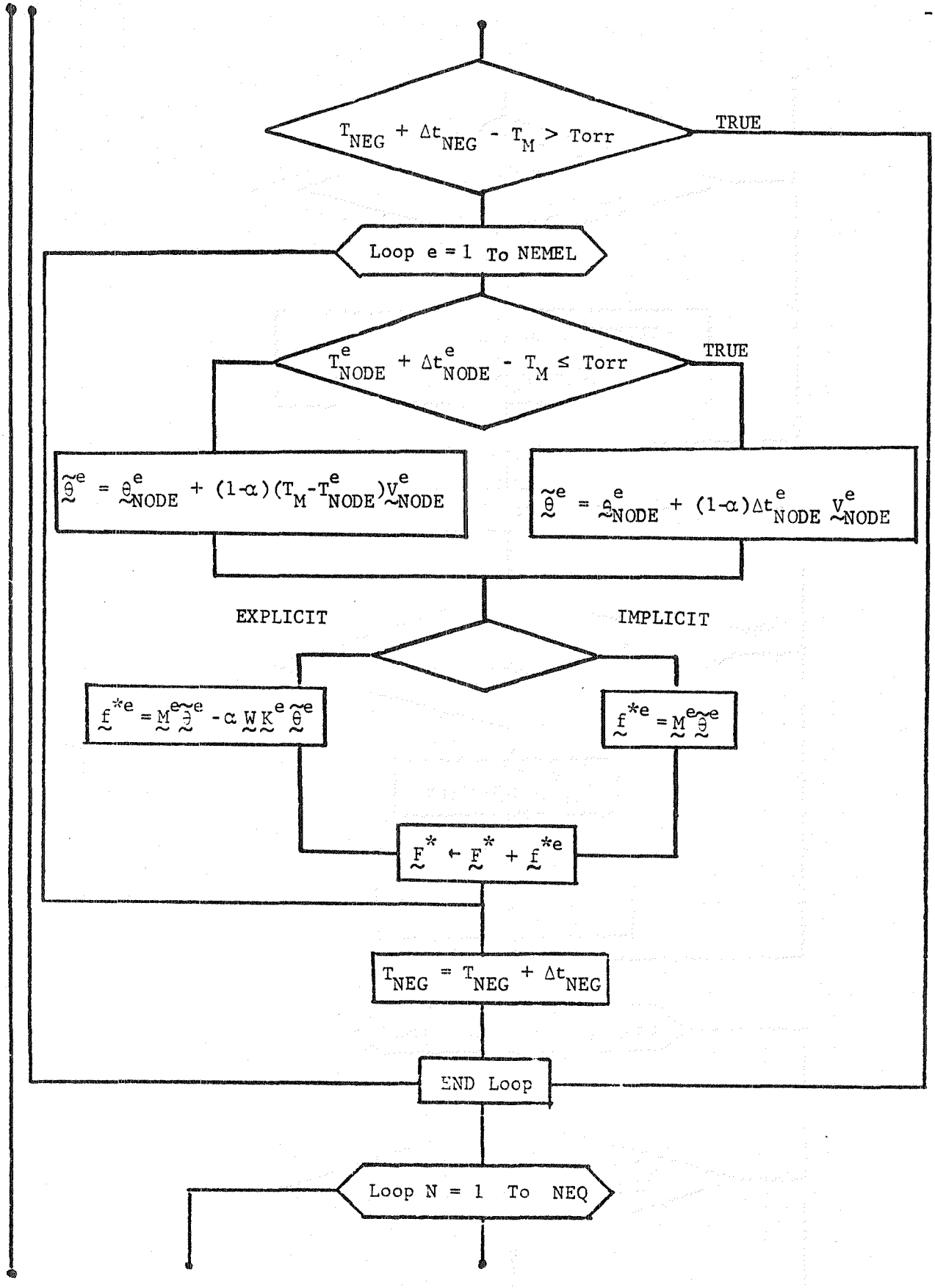
$T_{NEG} + \Delta t_{NEG} - T_M > Torr$
TRUE
Loop e = 1 To NEMEL
$T^e_{NODE} + \Delta t^e_{NODE} - T_M \leq Torr$
TRUE
$\tilde{\theta}^e = \theta^e_{NODE} + (1-\alpha)(T_M - T^e_{NODE})V^e_{NODE}$
$\tilde{\theta}^e = \theta^e_{NODE} + (1-\alpha)\Delta t^e_{NODE} V^e_{NODE}$
EXPLICIT
IMPLICIT
$f^{*e} = M^e \tilde{\theta}^e - \alpha W K^e \tilde{\theta}^e$
$f^{*e} = M^e \tilde{\theta}^e$
$F^* \leftarrow F^* + f^{*e}$
$T_{NEG} = T_{NEG} + \Delta t_{NEG}$
END Loop
Loop N = 1 To NEQ

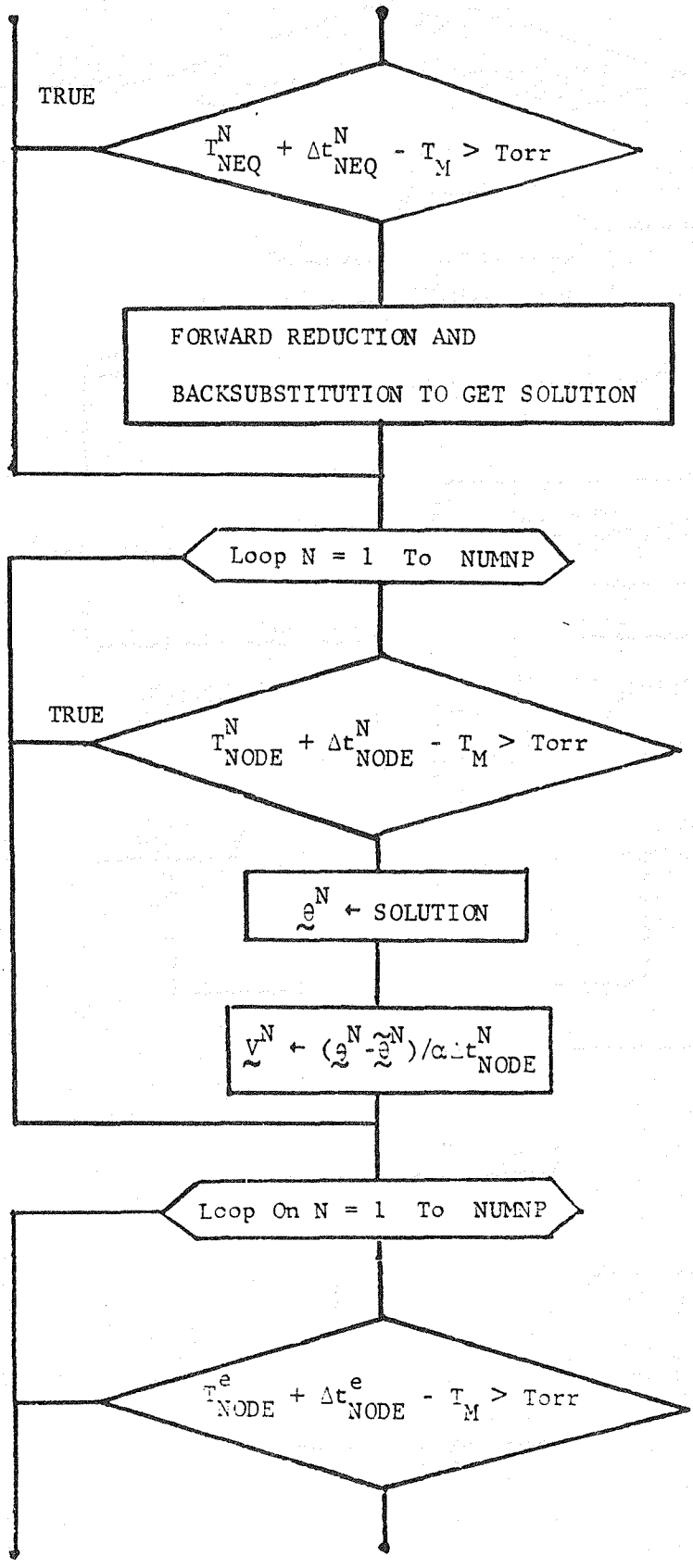
TRUE
$T^N_{NEQ} + \Delta t^N_{NEQ} - T_M > Torr$
FORWARD REDUCTION AND
BACKSUBSTITUTION TO GET SOLUTION
Loop N = 1 To NUMNP
TRUE
$T^N_{NODE} + \Delta t^N_{NODE} - T_M > Torr$
$\underset{\sim}{e}^N \leftarrow$ SOLUTION
$\underset{\sim}{V}^N \leftarrow (\underset{\sim}{e}^N - \underset{\sim}{\tilde{e}}^N)/\alpha \Delta t^N_{NODE}$
Loop On N = 1 To NUMNP
$T^e_{NODE} + \Delta t^e_{NODE} - T_M > Torr$

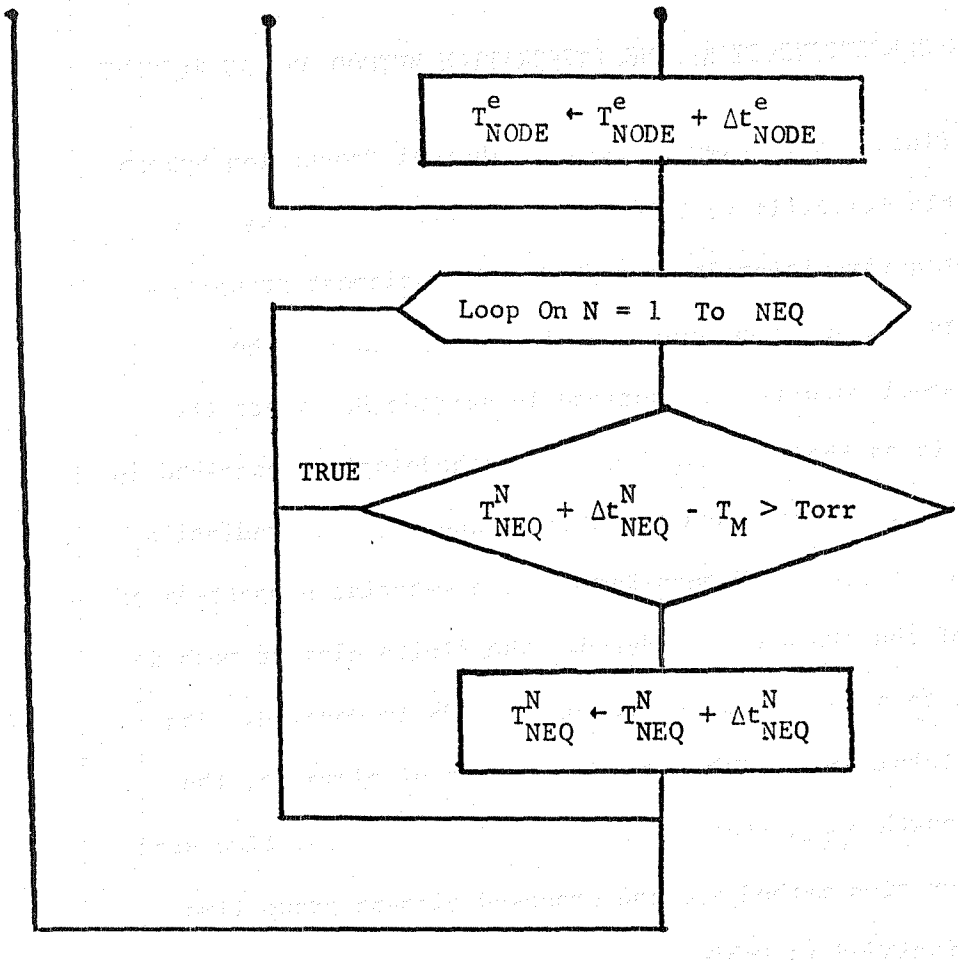
$T^{e}_{NODE} \leftarrow T^{e}_{NODE} + \Delta t^{e}_{NODE}$
Loop On N = 1 To NEQ
TRUE
$T^{N}_{NEQ} + \Delta t^{N}_{NEQ} - T_{M} > Torr$
$T^{N}_{NEQ} \leftarrow T^{N}_{NEQ} + \Delta t^{N}_{NEQ}$

7. ILLUSTRATION OF THE SELECTIONS OF A TIME INTEGRATION METHOD AND AN ELEMENT GROUP TIME STEP

A two dimensional finite element model for the Thermal Protection System (TPS) of the space shuttle [1] is formulated herein to illustrate the selection procedures for a time integration method and an element group time step. The practicability and usefulness of the algorithms can also be demonstrated with this model as will be described in section 8. Since the emphasis in this report is on the evaluation of the methodologies described in previous sections, nonlinear effects such as internal and external radiation are ignored. Further only the assumed mean temperature material properties of the various components of the TPS are considered. The finite element mesh is depicted in Fig. 5. Due to symmetry, only half of the TPS is modeled. Its material properties are tabulated in table 2. The number of elements, the minimum characteristic length ℓ_{min}, the estimated explicit critical time step Δt_{min}, the proposed integration method and the proposed element group time step for each group are included in table 3. As can be seen from table 3 due to the various thermal time scales (e.g. Δt_{min}=0.041 sec for AL, and Δt_{min}=16.71 sec for RSI), a single integration method is definitely not effective. For example, if an explicit method is employed, a time step of 0.041 sec has to be used; while if an implicit method is employed, there is no stability-imposed limitation on Δt; however, wide-banding bandwidth and/or demanding computer storage of the resulting matrix equations proportional to the square of bandwidth may decrease its advantage. The family of mixed time integration schemes developed is best suited for this type of problem. The attributes of the various time integration methods are fully achieved using the proposed approach as can readily be seen from table 3. It should also be observed that Δt_{min} can be set as high as 16.71 sec in this mixed model, the smallest time step required by an explicit group. Subsequently Δt=16.71 sec

is employed for element groups 1 and 2 (042 Coating and RSI), Δt=66.84 sec for element group 3 (RSI), and Δt=66.84 sec for element groups 4 and 5 (RTV, FELT, AL and AIR).

The advantage of this proposed mixed time implicit-explicit finite element concepts can further be visualized if a nonlinear analysis of the above finite element model is assumed. The thermal responses of the various components of the TPS may be divided into regions of slowly and rapidly varying temperatures and they are:

1. 042 Coating

   The thermal diffusivity is almost independent of temperature and the estimate Δt is so small (0.1225 sec) that explicit calculation is not cost effective at all. Implicit calculation is best suited since only limited partial reformation and refactorization of this element group's effective stiffness will be needed. This is one of the major advantages of the mixed time implicit-explicit concept.

2. RSI

   The thermal diffusivity changes rapidly with temperature, therefore reformation and refactorization of this element group's effective stiffness are frequently required if an implicit method is employed. Non-convergence and/or wide-banding of the resulting element group effective stiffness may decrease the advantage of applying the implicit method. The estimated Δt (based on mean temperature value) is 16.71 sec; therefore an explicit method is best suited (no matrices operations).

3. RTV

   Its thermal diffusivity is independent of temperature and the estimated Δt is so small (0.106 sec) that an implicit method is recommended.

Table 2. Mean Temperature Material Properties

MATERIAL / PROPERTIES	042 COATING	RSI	RTV	FELT	AL	AIR
λ w/m-K conductivity	1.4338	0.1354	0.3113	0.0363	13.5373	0.0271
ρ kg/m^3 density	1665.92	144.17	1409.62	96.11	2851.28	1.126
C J/kg-K specific heat	1317.96	1255.20	1213.36	1213.26	962.32	1009.0
$a=\frac{\lambda}{\rho C}$ m^2/sec thermal diffusivity	6.52×10^{-7}	7.48×10^{-7}	1.82×10^{-7}	3.11×10^{-7}	4.78×10^{-5}	2.39×10^{-5}

The mean temperature material properties are computed from the average of those at 1200 K, 950 K, 500 K, 477 K, 333 K and 300 K.

Table 3. Characteristic Length and Time Scales

ELEMENT GROUP NUMBER	MATERIAL TYPE	NUMBER OF ELEMENTS	L_{min}(cms)	ESTIMATED EXPLICIT Δt (sec)	INTEGRATION METHOD	ELEMENT GROUP TIME STEP (sec)
1	042 coating	12	0.04	0.1225	I	16.71 (=Δt)
2	RSI	30	0.5	16.71	E	16.71
3	RSI	18	1.04	72.29	E	66.84 (=4Δt)
4	RTV FELT AL	18 6 16	0.02 0.40 0.20	0.106 25.70 0.041	I	66.84
5	AIR	20	2.0	8.36	I	66.84

total number of elements = 120

I = implicit integration

E = explicit integration

4. AL

Its thermal diffusivity is fairly independent of temperature (at least in the operational temperature range of the space shuttle) and its estimated Δt is so stringent (0.041 sec) that an implicit method is again recommended.

5. FELT

Its thermal diffusivity is independent of temperature and its estimated Δt is large (25.7 sec), therefore implicit method or explicit method can be used. For this example, the implicit method is proposed. However for 3D calculation, in order to reduce the bandwidth and the unnecessary nonlinear calculations (due to the fact that the adjacent groups might be implicit groups too), explicit method will be recommended.

6. AIR

The variations of the thermal diffusivity with temperature are small in our range of interest. Also the estimated Δt is small, therefore implicit method is again well suited.

Remarks:

(1) In the above Δt calculations, $\ell_{min} = \min\{\ell_x, \ell_y\}$ where ℓ_x and ℓ_y are defined in section 5.

(2) The estimated Δt is defined to be $\ell_{min}^2/2a$. It is a safe critical time step calculation. See [13-14] for a discussion.

(3) By virtue of the fact that each element group's effective stiffness is uncoupled to the global assembled matrix equations system, any element group can be reformed and refactorized at any instant if required without affecting the global equations system. This partial factorization procedure can further be enhanced if it is to be combined with an iterative update procedure.

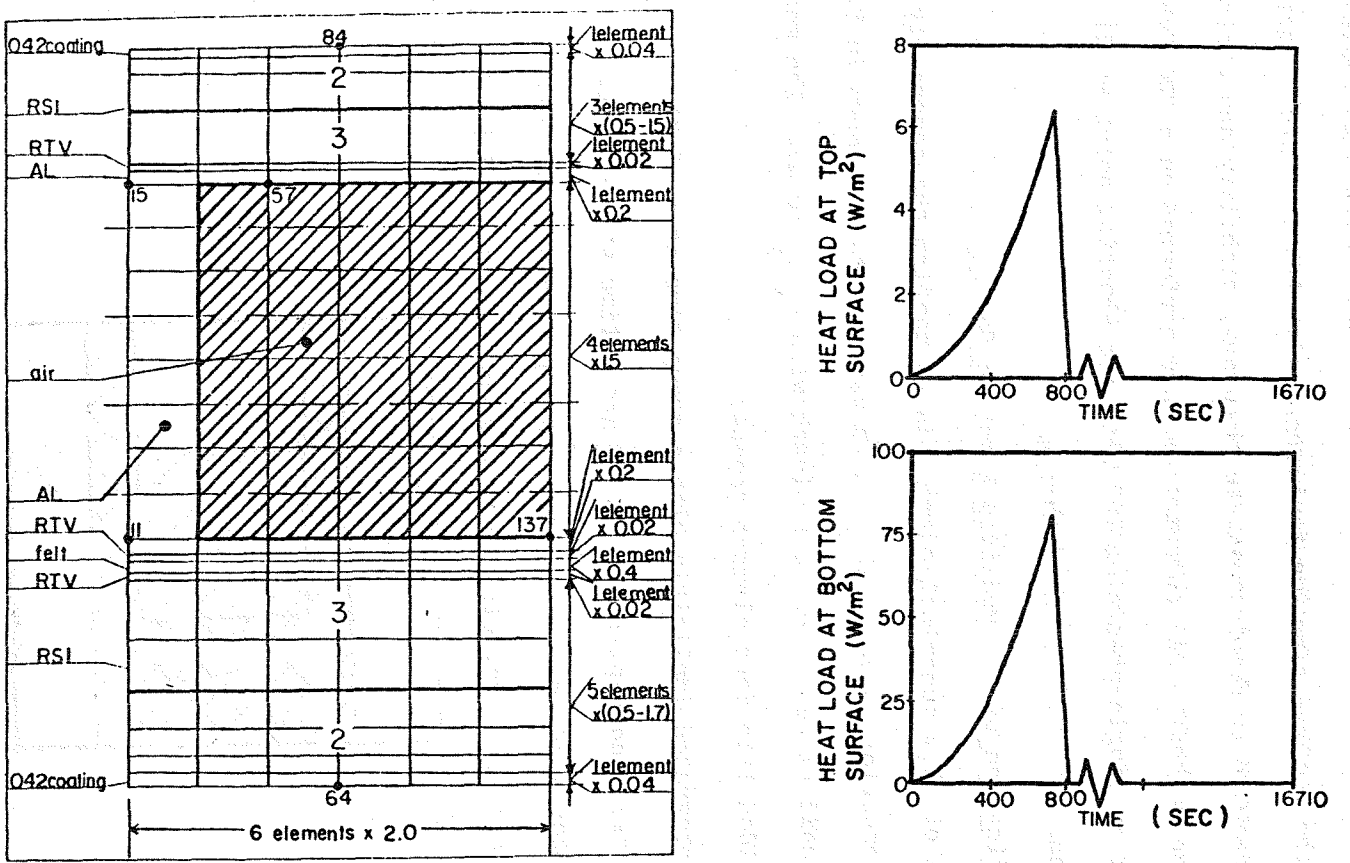

Fig. 5. Problem statement and finite element mesh of a two-dimensional thermal protection systems (TPS)

8. NUMERICAL RESULTS

A two dimensional finite element pilot computer code incorporating the methodologies described in previous sections has been written to evaluate the performance of these mixed time finite element algorithms. Three numerical examples are presented to demonstrate the accuracy, stability and efficiency of these proposed methods. All computations are performed on a CDC Cyber 170/730 computer in single precision (60 bits per floating point word) and lumped capacitance matrices are used throughout.

Example 1 Verification of the Modified Equation Solver

The purpose of this numerical example is to confirm the generality of the modified column equation solver. The finite element mesh as shown in Fig. 6 consists of 100 uniform square elements (each with $\ell_x=\ell_y=10$ m). The mesh is deliberately divided into four element groups:

1) Group 1 is integrated implicitly with a group time step of $2\Delta t$.
2) Group 2 is integrated explicitly with a group time step of $2\Delta t$.
3) Group 3 is integrated implicitly with a group time step of $4\Delta t$.
4) Group 4 is integrated explicitly with a group time step of Δt.

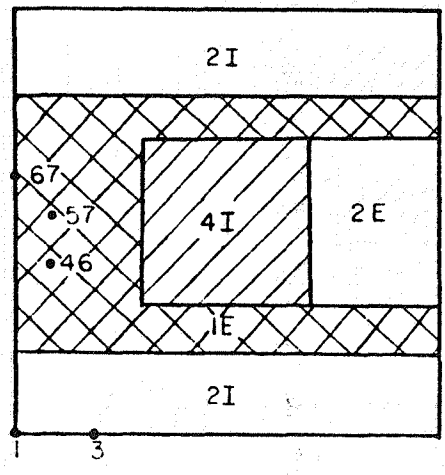

Fig. 6. Problem statement and finite element mesh of numerical example 1

The above partition is called a 2I-2E-4I-1E partition. Observed that group 3 (4I) is chosen to be at the center of the square. As described in [8,13-14], the variable column heights (which affect the solution time) depend on the nodal numbering. Furthermore, no forward reduction and backsubstitution are performed until every $4\Delta t$ time interval. As can be pictured from Fig. 6, the column heights of the "$4\Delta t$" equations are coupled to the "Δt" and "$2\Delta t$" equations, therefore unlike the one dimensional case (see [14] for a discussion) a special forward reduction and backsubstitution procedure as described in section 6 is required for efficiency.

The thermal diffusivity a is chosen to be 6.25 m^2/sec for all the elements. Node 1 is kept at a constant temperature of 0.0 ^oC while all the other nodes are subjected to a constant initial temperature of 0.1 ^oC. All four sides are insulated. A time step of Δt equal to 1 sec is employed for the transient analysis. The temperature-time histories of nodes 3, 46, 57 and 67 are depicted in Fig. 7. In order to confirm the accuracy of these solutions, the mixed time finite element solutions are compared to those obtained using a finite difference 21×21 (400 zones) grid with a single time step of Δt equal to 1 sec. The finite difference solutions of these four nodes are also depicted in Fig. 7. As can be seen, the comparison is quite good despite the crudeness of the mesh (as compared to the finite diference method) and the larger time steps used in the finite element mesh (1 as compared to 1, 2, and 4 for groups 4, 1 and 2, and 3 respectively). The maximum relatively difference between the two solutions is no more than 2%.

Example 2 Demonstration of Accuracy, Stability and Efficiency

The purpose of this numerical example is to evaluate the performance of this mixed time implicit-explicit method as compared to an implicit method. The problem statement is depicted in Fig. 8. The finite element mesh consists

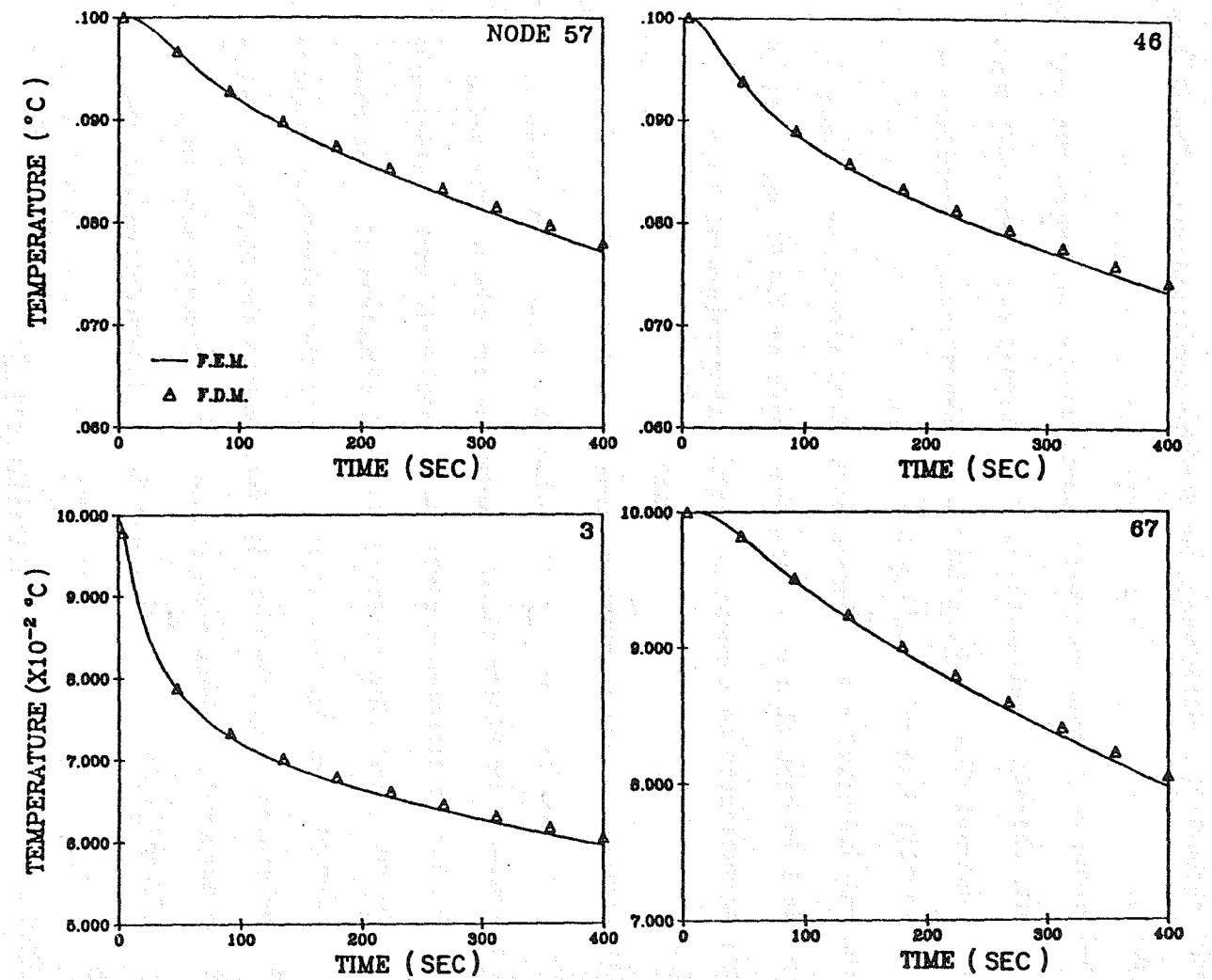

Fig. 7. Comparison between finite element and finite difference solutions

of 400 uniform size rectangular elements (each has ℓ_x=5 m and ℓ_y=10 m) and 486 nodes (81 in x direction and 6 in y direction) where the x-axis is defined by joining node 3 to node 17. The material properties of this finite element model are composed of four different thermal diffusivities of 0.125a, 0.25a, a and 40a respectively as shown in Fig. 8. a is chosen to be 12.5 m^2/sec. In order to simulate a realistic three dimensional bandwidth using this two dimensional finite element model, the nodes are numbered sequentially along the x-axis. The heat load which is also shown in Fig. 8 is applied at node 1. The initial temperature for all the nodes is 0.1 ^oC. All four sides are insulated.

As mentioned earlier, due to the different thermal diffusivities, a single time integration method is inefficient for this problem. For example, if explicit method is employed, a time step of 0.025 sec is required so that 16,000 steps (as compared to 400 steps) are required for this problem. Therefore purely explicit integration method is not being considered here. If implicit method is employed, a much larger time step can be employed though the wide bandwidth and demanding computer storage (e.g. 3288 vs. 33771 single precision words) may decrease the advantage of the implicit method. This can readily be seen in table 4. Hence mixed time implicit-explicit method is best suited for this example. A total of five computer runs are made to demonstrate the accuracy, stability and efficiency of the proposed mixed time methods and they are:

(1) 1E-4E-8I-8E with Δt=1 sec.

(2) 1I with Δt=1 sec.

(3) 1I-1E-2I-2E with Δt=4 sec.

(4) 1I with Δt=4 sec.

(5) 1I with Δt=8 sec.

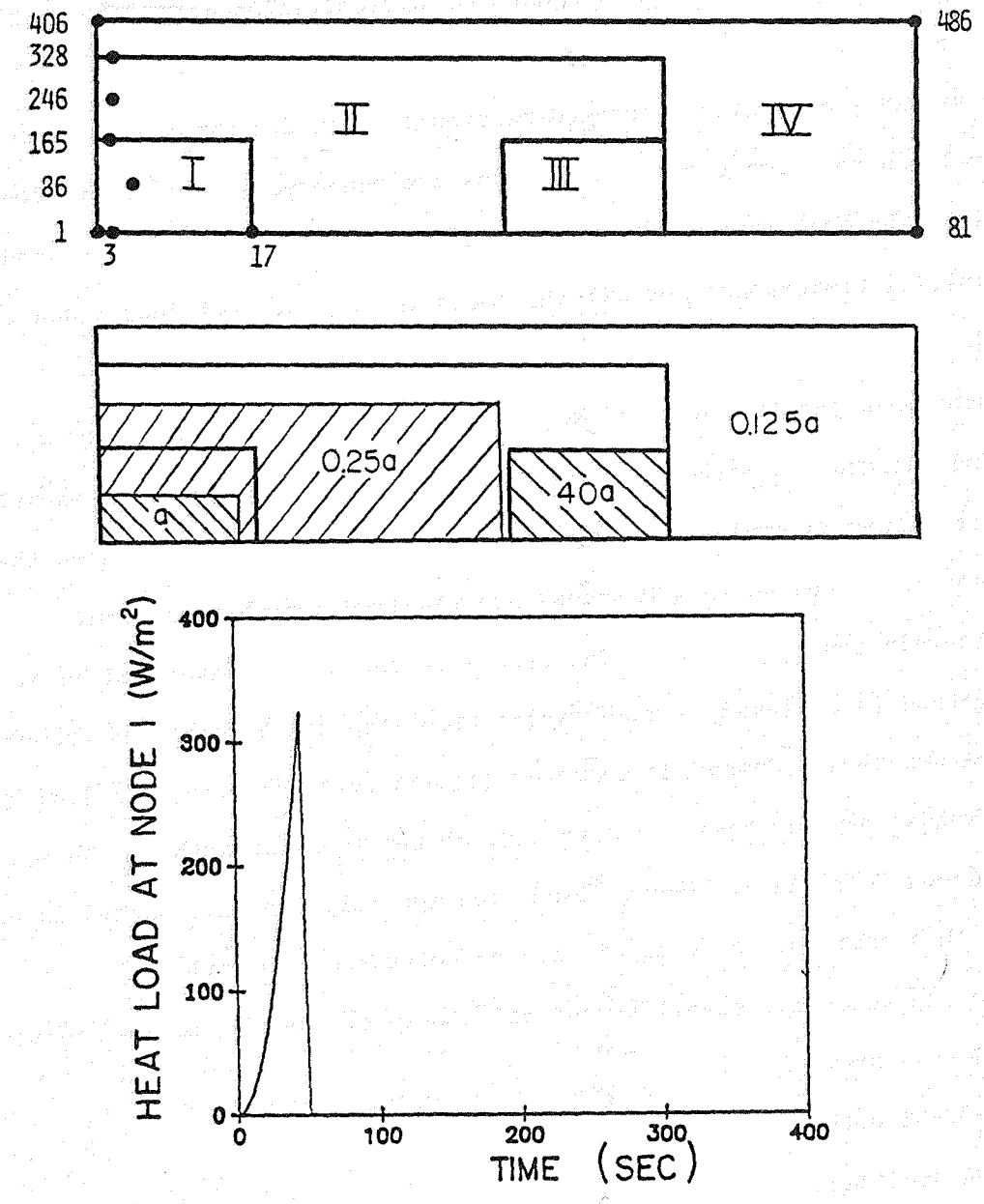

Fig. 8. Problem statement and finite element mesh of numerical example 2

Table 4. Storage (in Single Precision Words

Method / Item	1E-4E-8E-8I (Δt=1 sec)	1I (Δt=1 sec)	1I-1E-2E-2I (Δt=4 sec)	1I (Δt=4 sec)	1I (Δt=8 sec)
Number of equations (NEQ)	486	486	486	486	486
Number of Terms in Stiffness (NA)	3288	33771	6089	33771	33771
Average Half Bandwidth $MB \stackrel{def}{=} NA/NEQ$	6	69	12	69	69

Table 5. Solution Times (in Seconds)

Method / Item	1E-4E-8E-8I (Δt=1 sec)	1I (Δt=1 sec)	1I-1E-2E-2I (Δt=4 sec)	1I (Δt=4 sec)	1I (Δt=8 sec)
Formulation of Stiffness and Load	78.96	211.13	58.13	52.98	28.81
Factorization	0.34	11.21	0.80	11.55	11.53
Forward Reduction and Backsubstitution	10.95	293.58	10.90	74.24	37.50
Total Solution Time	90.25	515.92	69.83	138.77	77.84

In run 1, groups I, II and IV are integrated explicitly with 1E, 4E and 8E respectively; and group III is integrated implicitly. In run 3, groups II and IV are integrated explicitly with 1E and 2E respectively; while groups I and III are integrated implicitly with 1I and 2I respectively. The time step Δt and the element group time steps are chosen according to the critical time step formula given in section 5 with μ equal to 1.0. The temperature-time histories at six different locations for run number 1, i.e. 1E-4E-8I-8E, are presented in Fig. 9. These results are virtually identical to those obtained from run number 2, i.e. 1I. It should be pointed out that the curves shown in Fig. 9 are plotted for every time interval of 4 except for run number 5 in which the time interval is 8. Since the plot of node 327 is integrated with a time step of 8, therefore the temperature time history shown is "step-wise" (from time $\approx$ 48 to 240 sec). The storage requirements and solution times for the above five runs are tabulated in tables 4 and 5 respectively. From these tables, the advantages of these mixed time integration methods are apprarent. The relative accuracy of these five runs are compared and they are shown in Fig. 10. These curves are plotted at every time interval of 8 sec. In summary, from accuracy consideration, runs 1 and 3 made with the mixed time implicit-explicit method, are comparable to runs 2 and 4 made with an implicit method but with two different time steps. Run 5, also an implicit method but utilizing a larger time step, was not as accurate as the others. Runs 1 and 3 required 10% and 18% respectively of the storage required by run 4 and 65% and 50% respectively of computational time of run 4. The potential savings in both computer time and computer storage will be even greater in three dimensional and/or nonlinear calculations. Finally, the critical time step estimate is also confirmed by this numerical example.

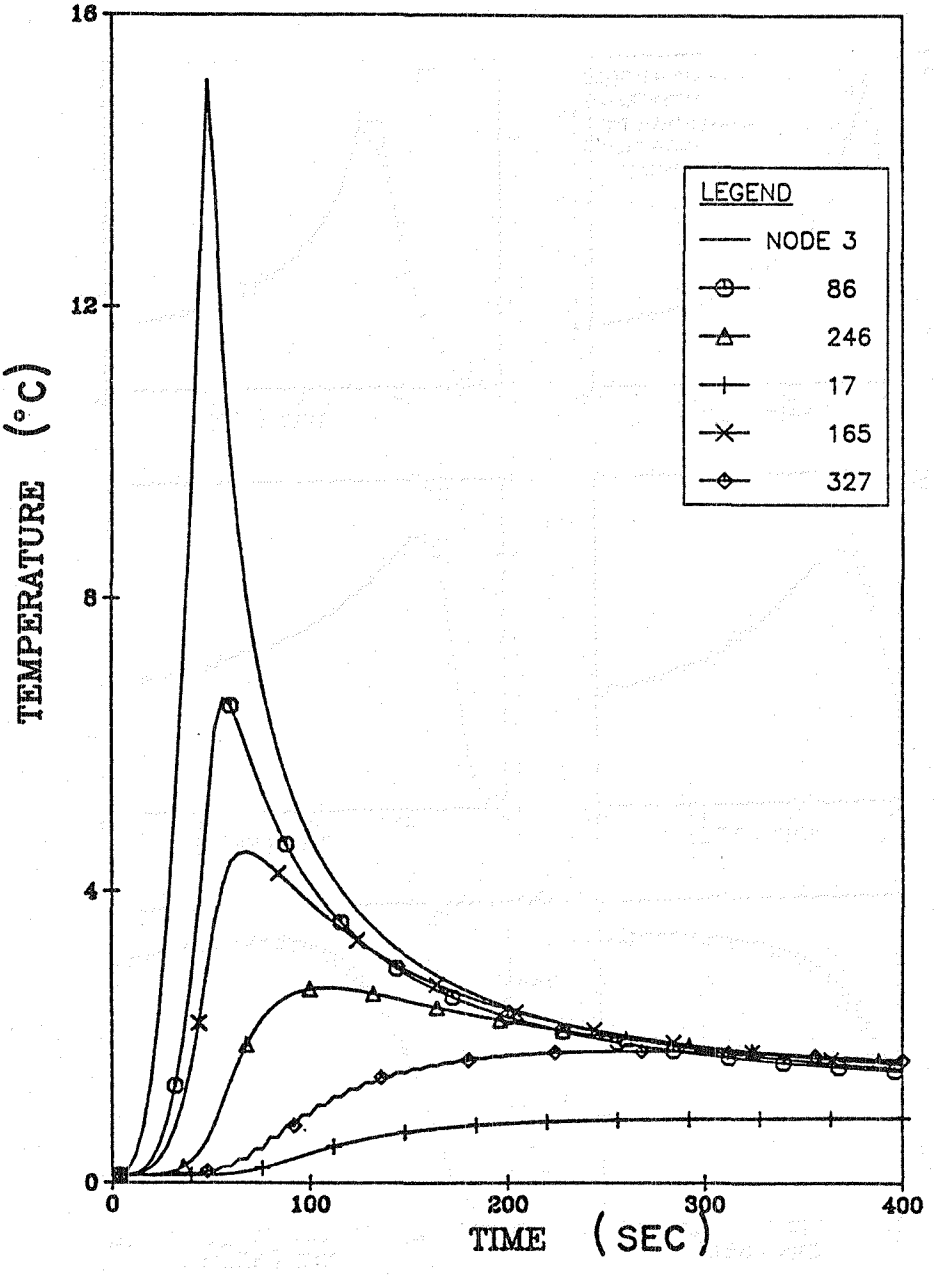

Fig. 9. Time histories at selected nodes for example 2 with E-4E-8I-8E integration

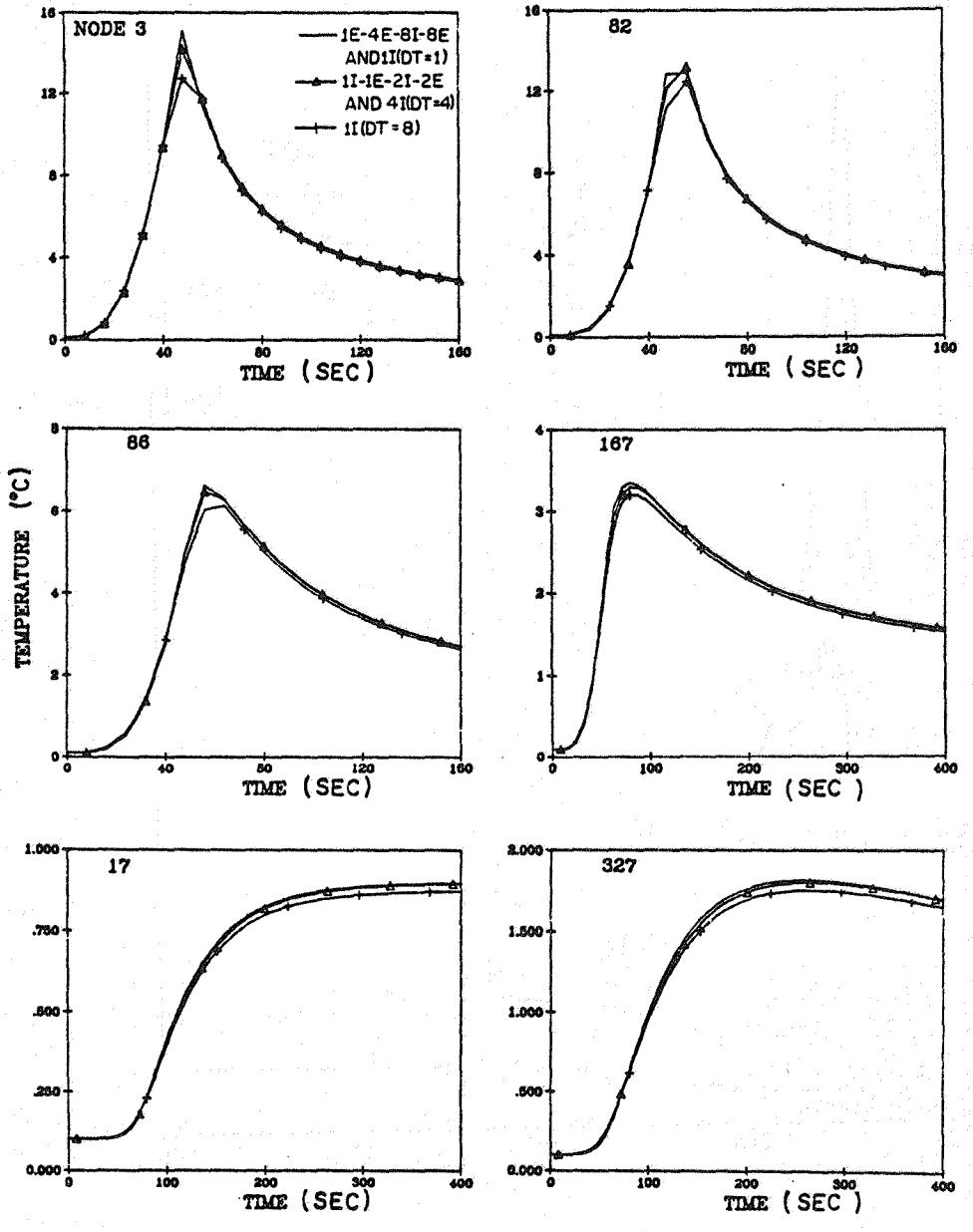

Fig. 10. Comparison of solutions of five integration methods

Example 3 Applications to TPS

The purpose of this numerical example has been described in section 7. Two integration methods are employed to compute the time histories of the top (node 84) and bottom (node 64) surface temperatures of the 042 coatings andthe lower (nodes 11 and 137) and upper (nodes 15 and 57) aluminum skin temperatures for the two dimensional finite element model described in section 7. Its dimensions (not to scale and in cms) are depicted in Fig. 5. The heat loads which are also shown in Fig. 5 are applied at the top and bottom of the TPS model. The initial temperature for all the nodes is -20 ^{o}C. Sides AD and BC are symmetry planes.

From the data given in section 7, 407561 time steps (as compared to 1000 steps) are required if purely explicit method is employed. Therefore, purely explicit time integration method is not being considered. The 1I-1E-4E-4I-4I time integration with a time step of 16.71 sec for the 042 coating and part of RSI, and a time step of 66.84 sec for the other part of RSI, RTV, FELT, AL and AIR is proposed. The computed results are then compared to those using purely implicit method with a single time step of 16.71 sec. The temperature-time histories (plotted at every time interval of 66.84 sec) at six different locations (042 coatings and aluminum skin) are presented in Fig. 11. These results are virtually identical to those obtained from the purely implicit case, i.e. 1I. The closed up temperature-time histories at four different locations are given in Fig. 12. These curves are plotted at every time interval of 16.71 sec for a time period of about 4000 sec. The solution times and computer storage requirements for these two runs are tabulated in tables 6 and 7 respectively. Eventhough only a total of 147 nodes and 120 elements (a very small mesh as compared to a typical 3D finite element model of 3000 nodes and 4000 elements) is used, a factor of about 1.7 in solution time and a

factor of about 1.5 in computer storage are gained. Again, the advantages as well as the stability of these mixed time methods are fully illustrated.

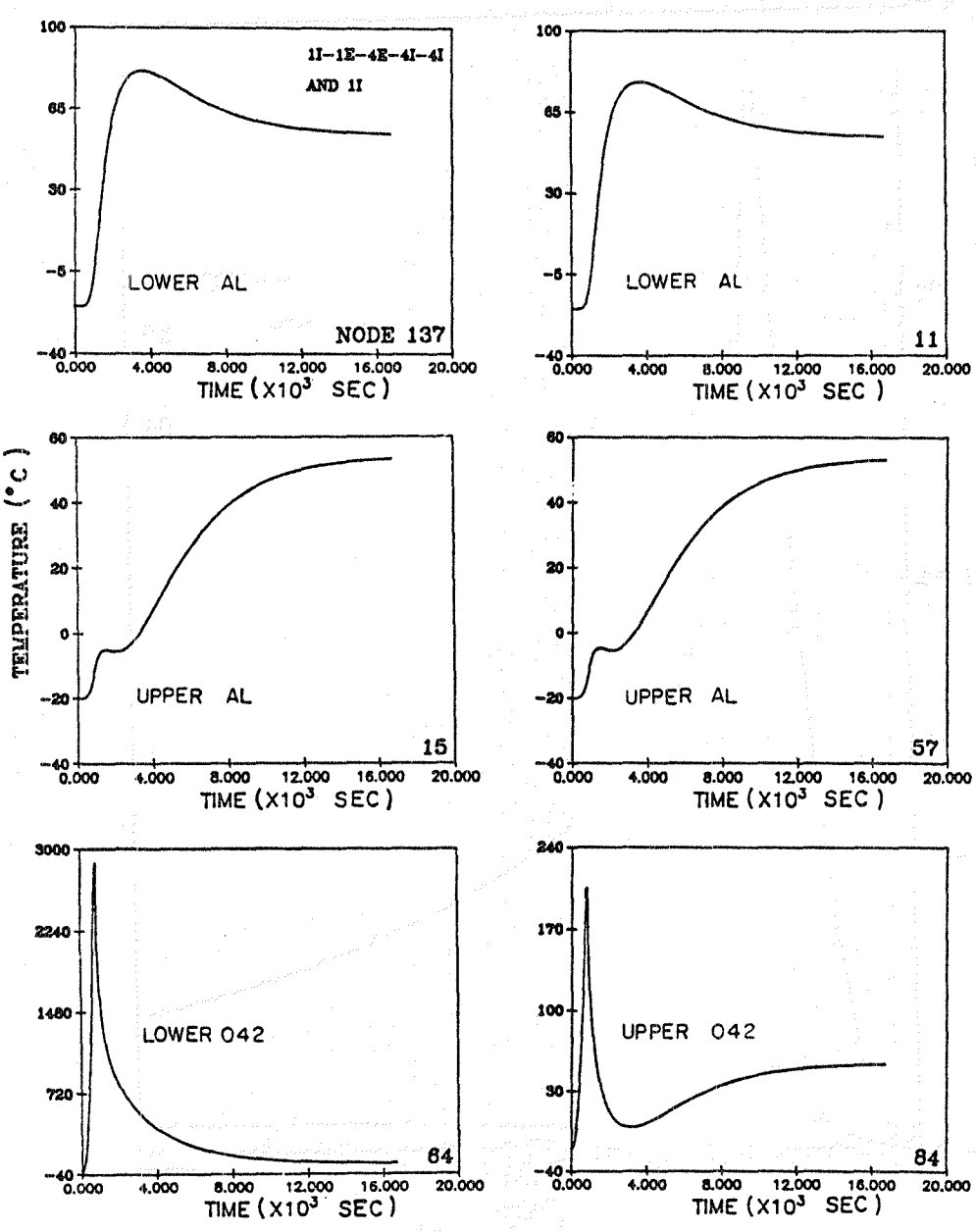

Fig. 11. Comparison of solutions of two integration methods

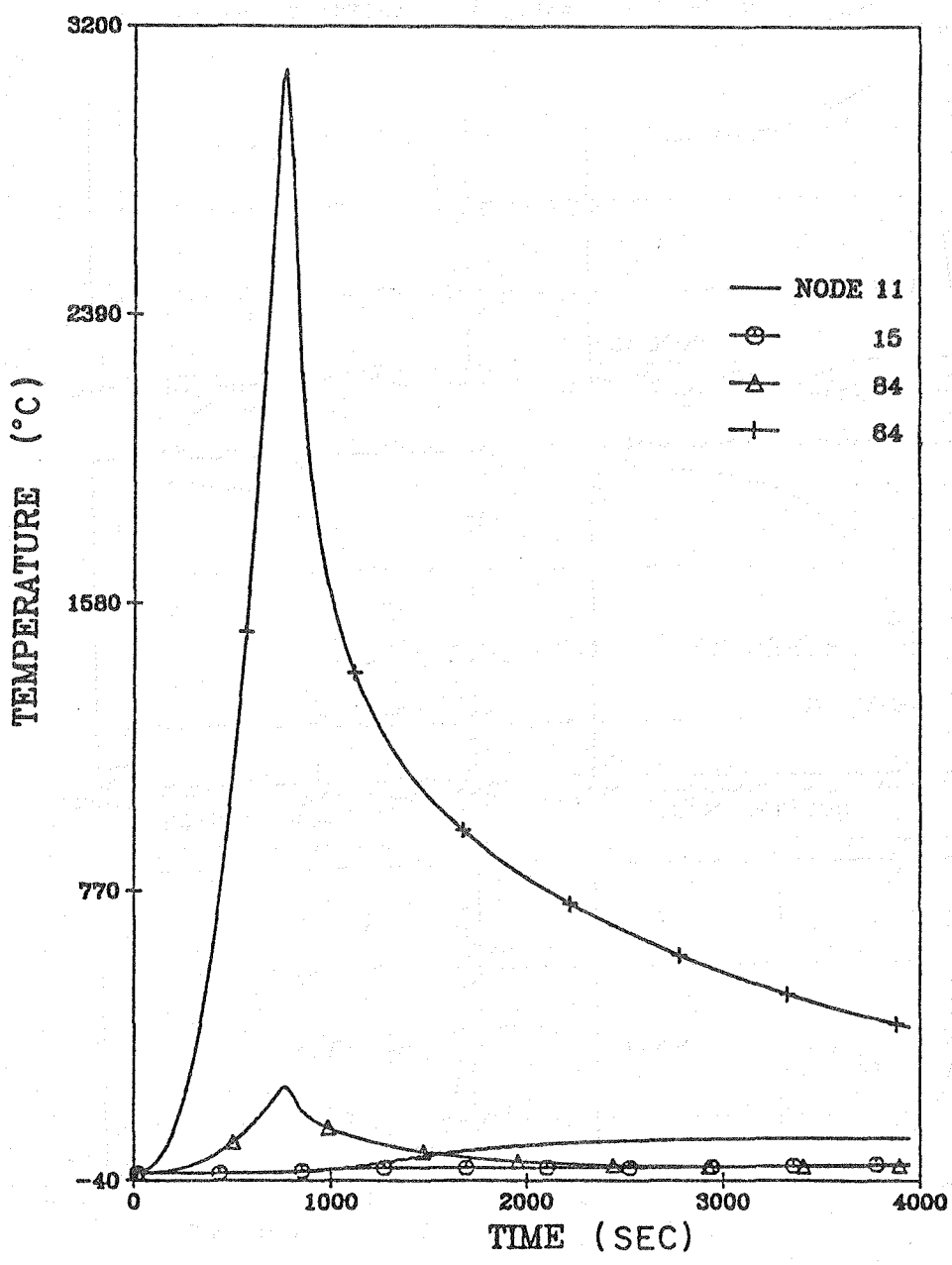

Fig. 12. Closed up temperature time histories at four different locations

Table 6. Solution Times (in Seconds)

Item \ Method	1I-1E-4E-4I-4I (Δt=16.71 sec)	1I (Δt=16.71 sec)
Formulation of Stiffness and Load	105.12	162.54
Factorization	0.36	0.57
Forward Reduction and Backsubstitution	45.05	91.00
Total Solution Time	160.42	263.35

Table 7. Storage (in Single Precision Words)

Item \ Method	1I-1E-4E-4I-4I (Δt=16.71 sec)	1I (Δt=16.71 sec)
Number of equations (NEQ)	147	147
Number of Terms in Stiffness (NA)	2121	2933
Average Half Bandwidth $MB \stackrel{def}{=} NA/NEQ$	14	19

9. CONCLUSIONS

The computer implementation aspects; stability criterion and the evaluation of the performance of mixed time implicit-explicit finite element as applied to multidimensional transient thermal analysis are presented. The report focuses on applications where the thermal model would normally have different time scales of thermal response. Three two-dimensional examples are presented to illustrate the approach: (1) comparison with finite difference method, (2) demonstration of accuracy, stability and efficiency and (3) application to Thermal Protection Systems. The examples show: (1) the superiority of mixed time methods to a single integration method (either implicit or explicit), (2) potential savings in computer time and computer storage, and (3) the accuracy and stability behavior of mixed time finite element.

REFERENCES

1. H. N. Kelly; D. R. Rummler; and R. L. Jackson: Research in Structures and Materials for Future Space Transportation Systems - An Overview. Presented at the AIAA Conference on Advanced Technology for Future Space Systems, May 8-11, 1979, Langley Research Center, Hampton, Virginia, AIAA Paper No. 79-0859.

2. J. L. Shideler; H. N. Kelly; M. L. Blosser; and H. M. Adelman: Multiwall TPS - An Emerging Concept. AIAA/ASME/ASCE/AHS 22nd Structures, Structural Dynamics and Materials Conference, April 6-8, 1981, Atlanta, Georgia.

3. R. J. Jackson; and S. C. Dixon: A Design Assessment of Multiwall, Metallic Stand-Off and RSI Reusable Thermal Protection System Including Space Shuttle Applicatons. NASA TM 81780, April 1980.

4. W. Blair; J. E. Meany; and H. A. Rosenthal: Design and Fabrication of Titanium Multiwall Thermal Protection System (TPS) Test Panels, NASA CR 159241, February 1980.

5. H. Adelman; and R. Haftka: On the Performance of Explicit and Implicit Algorithms for Transient Thermal Analysis of Structures. NASA TM 81880, September 1980.

6. SPAR Structural Analysis System Reference Manual, Vol. 1, NASA CR 158970-1, December 1978.

7. T. Belytschko; and R. Mullen: Stability of Explicit-Implicit Mesh Partition in Time Integration. International Journal Numerical Method in Eng. 12, 1575-1586, 1978.

8. T. Hughes; and W. Liu: Implicit-Explicit Finite Elements in Transient Analysis. Journal Applied Mechanics 45, 371-378, 1978.

9. W. Liu: Development of Finite Element Procedures for Fluid-Structure Interactions. EERL 80-06, California Institute of Technology, Pasadena, California, August 1980.

10. T. Hughes; W. Liu; and A. Brooks: Review of Finite Element Analysis of Incompressible Viscous Flows by the Penalty Function Formulation. Journal Computational Physics 30, 1-60, 1979.

11. T. Belytschko; and R. Mullen: Explicit Integration of Structural Problems. In P. Bergan et. al., (eds.) Finite Elements in Nonlinear Mechanic, 2, 697-720, 1977.

12. T. Belytschko: Partitioned and Adaptive Algorithms for Explicit Time Integration. In the book of Nonlinear Finite Element Analysis in Structural Mechanics, edited by W. Wunderlich et. al., Springer-Verlag, Berlin, July 1980.

13. W. Liu; and T. Belytschko: Mixed Time Implicit-Explicit Finite Element for Transient Analysis. Computers and Structures, Vol. 15, 1982, pp. 445-450.

14. W. Liu; and J. Lin: Stability of Mixed Time Integration Schemes for Transient Thermal Analysis. Numerical Heat Transfer Journal, Vol. 5, 1982, pp. 211-222.

1. Report No.	2. Government Accession No.	3. Recipient's Catalog No.
NASA CR-172209		

4. Title and Subtitle	5. Report Date
MIXED TIME INTEGRATION METHODS FOR TRANSIENT THERMAL ANALYSIS OF STRUCTURES	September 1983
	6. Performing Organization Code
7. Author(s)	8. Performing Organization Report No.
Wing Kam Liu	
	10. Work Unit No.
9. Performing Organization Name and Address	
Northwestern University Department of Mechanical and Nuclear Engineering Evanston, IL 60201	11. Contract or Grant No. NAG1-210
	13. Type of Report and Period Covered Contractor Report 10-1-81 - 9-30-82
12. Sponsoring Agency Name and Address	
National Aeronautics and Space Administration Washington, DC 20546	14. Sponsoring Agency Code

15. Supplementary Notes

Langley Technical Monitor: George C. Olsen
Final Report

16. Abstract

The computational methods used to predict and optimize the thermal-structural behavior of aerospace vehicle structures are reviewed. In general, two classes of algorithms, implicit and explicit, are used in transient thermal analysis of structures. Each of these two methods has its own merits. Due to the different time scales of the mechanical and thermal responses, the selection of a time integration method can be a difficult yet critical factor in the efficient solution of such problems.

Therefore mixed time integration methods for transient thermal analysis of structures are being developed. The computer implementation aspects and numerical evaluation of these mixed time implicit-explicit algorithms in thermal analysis of structures are presented. A computationally-useful method of estimating the critical time step for linear quadrilateral element is also given. Numerical tests confirm the stability criterion and accuracy characteristics of the methods. The superiority of these mixed time methods to the fully implicit method or the fully explicit method is also demonstrated.

17. Key Words (Suggested by Author(s))	18. Distribution Statement
Implicit Explicit Implicit-explicit Mixed time Transient thermal analysis Thermal response Critical time step	Unclassified - Unlimited Subject Category 64

19. Security Classif. (of this report)	20. Security Classif. (of this page)	21. No. of Pages	22. Price
Unclassified	Unclassified	55	A04

For sale by the National Technical Information Service, Springfield, Virginia 22161

End of Document